LHCb-CONF-2024-004
July 26, 2024

Simultaneous determination of the CKM angle γ and parameters related to mixing and *CP* violation in the charm sector

LHCb collaboration[†]

Abstract

A combination of measurements sensitive to the *CP*-violation angle γ of the Cabibbo–Kobayashi–Maskawa unitarity triangle, to the charm mixing parameters that describe oscillations between D^0 and $\overline{D}^0$ mesons, and to the *CP* asymmetries in the $D^0 \to K^+K^-$ and $D^0 \to \pi^+\pi^-$ decays is performed. All relevant beauty and charm results obtained with the data collected with the LHCb detector at CERN's Large Hadron Collider to date are included. The charm mixing parameters are determined to be $x = (0.41 \pm 0.05)\%$ and $y = (0.621\,^{+0.022}_{-0.021})\%$, the magnitude and phase of *CP* violation in charm mixing to be $|q/p| = 0.989 \pm 0.015$ and $\phi = (-2.5 \pm 1.2)^\circ$, and the *CP* asymmetries in decay to be $a^{\rm d}_{K^+K^-} = (6\,^{+6}_{-5}) \times 10^{-4}$ and $a^{\rm d}_{K^+K^-} = (22 \pm 6) \times 10^{-4}$, with a correlation of $\rho = 0.88$. The angle γ is found to be $(64.6 \pm 2.8)^\circ$, which is the most precise determination from direct measurements to date.

[†]Conference report prepared for the 42nd International Conference on High Energy Physics, Prague, Czech Republic, 17–24 July 2024. Contact authors: Jordy Butter, jordy.butter@cern.ch Alex Gilman, alexander.leon.gilman@cern.ch Matthew Kenzie, matthew.william.kenzie@cern.ch, Tommaso Pajero, tommaso.pajero@cern.ch, Mark Whitehead, mark.peter.whitehead@cern.ch.

1 Introduction

Precise measurements of the Cabibbo–Kobayashi–Maskawa (CKM) unitarity triangle provide a strict test of the Standard Model (SM) and allow for indirect searches for physics beyond the SM (BSM) in the quark sector up to very high mass scales. The CP-violating phase $\gamma \equiv \arg(-V_{ud}V_{ub}^*/V_{cd}V_{cb}^*)$, where $V_{qq'}$ is the CKM matrix element for the quarks q and q', is the only angle of the unitarity triangle that can be determined using solely measurements of tree-level B-meson decays [1–8]. Assuming no new physics at tree level [9], the theoretical uncertainties are negligible in such direct measurements [10]. Deviations between direct measurements of γ and indirect determinations from global CKM fits [11, 12], which are based on independent observables and assume the validity of the SM and hence unitarity of the CKM matrix, would be a clear indication of physics BSM. Furthermore, comparisons between the values of γ measured using decays of different B-meson species provide sensitivity to possible BSM effects at the tree level given the different topologies of the involved decay amplitudes. For example, modes involving a charged initial state have sensitivity to annihilation diagrams that the neutral modes do not. The world average for direct measurements of $\gamma = (66.5^{+2.8}_{-2.9})^\circ$ [13] is dominated by LHCb results [14]. The experimental uncertainty on γ is larger than the indirect determination obtained from global CKM fits, $\gamma = (66.3^{+0.7}_{-1.9})^\circ$ using a frequentist framework [11], and $\gamma = (64.9 \pm 1.4)^\circ$ with a Bayesian approach [15]. Closing this sensitivity gap is a key physics goal of the LHCb experiment [16, 17].

This note updates the combination of measurements of the angle γ and of mixing and CP violation in D^0–$\overline{D}^0$ mixing presented in Refs. [14, 18]. It includes nine new measurements published by the LHCb collaboration during 2023 and 2024 [19–27]. The statistical procedure is identical to that described in Ref. [18], and follows a frequentist treatment described in detail in Ref. [28]. The formalism, motivation and implementation of this update follow those described in Ref. [18], and the results presented here supersede previous LHCb combinations [14, 18, 28–34].

2 Input measurements and assumptions

The full list of LHCb measurements that are used as inputs to the present combination is provided in Table 1. Additional external constraints for the hadronic parameters and coherence factors in multibody B and D decays are summarised in Table 2. Compared to the previous combination [14], there are four new and three updated measurements from beauty meson decays and one new measurement and one updated measurement of charm meson decays.

For the beauty inputs, the first new result is a measurement of $B^\pm \to Dh^\pm$ with $D \to h^+h^-\pi^+\pi^-$ decays [19], from which only the model-independent phase-space integrated results are included.[1] The next two are measurements of $B^\pm \to D^*h^\pm$ with $D \to K^0_S h^+h^-$ decays in which the D^* meson is either partially [20] or fully reconstructed [21]. The fourth is a measurement of $B^\pm \to DK^{*\pm}$ with $D \to h^\pm h'^\mp$, $D \to h^\pm\pi^\mp\pi^+\pi^-$, and $D \to K^0_S h^+h^-$ decays [22]. The three remaining beauty inputs are updated measurements of $B^0 \to DK^{*0}$ with $D \to h^\pm h'^\mp$ and $D \to h^\pm\pi^\mp\pi^+\pi^-$ [23]

[1] Throughout the note, $h^\pm$ and $h'^\pm$ are used to refer to $\pi^\pm$ or $K^\pm$, D to refer to a superposition of D^0 and $\overline{D}^0$ states, and D^* to a superposition of D^{*0} and $\overline{D}^{*0}$ states.

Table 1: Measurements used in the combination. Those that are new or have changed since the previous combination [14] are highlighted in bold. LHCb Run 1 took place from 2011 to 2012, collecting proton-proton collision data at centre-of-mass energies, $\sqrt{s}$, of 7 and 8 TeV, corresponding to an integrated luminosity of 1 and 2 fb^{-1}, respectively. LHCb Run 2 took place from 2015 to 2018 at $\sqrt{s} = 13$ TeV, corresponding to an integrated luminosity of 6 fb^{-1}. In the table, "PR" refers to measurements where the γ or π^0 from $D^* \to \gamma/\pi^0 D$ decays is not reconstructed, and "FR" refers to measurements where a $D^* \to \gamma/\pi^0 D$ candidate is fully reconstructed. Where multiple references are cited, measured values are taken from the most recent results, which include information from the others.

B decay	D decay	Ref.	Dataset	Status since Ref. [14]
$B^\pm \to Dh^\pm$	$D \to h^\pm h'^\mp$	[35]	Run 1&2	*As before*
$B^\pm \to Dh^\pm$	$D \to h^+h^-\pi^+\pi^-$	[19]	Run 1&2	**New**
$B^\pm \to Dh^\pm$	$D \to K^\pm\pi^\mp\pi^+\pi^-$	[36]	Run 1&2	*As before*
$B^\pm \to Dh^\pm$	$D \to h^\pm h'^\mp\pi^0$	[37]	Run 1&2	*As before*
$B^\pm \to Dh^\pm$	$D \to K^0_S h^+h^-$	[38]	Run 1&2	*As before*
$B^\pm \to Dh^\pm$	$D \to K^0_S K^\pm\pi^\mp$	[39]	Run 1&2	*As before*
$B^\pm \to D^*h^\pm$	$D \to h^\pm h'^\mp$ (PR)	[35]	Run 1&2	*As before*
$B^\pm \to D^*h^\pm$	$D \to K^0_S h^+h^-$ (PR)	[20]	Run 1&2	**New**
$B^\pm \to D^*h^\pm$	$D \to K^0_S h^+h^-$ (FR)	[21]	Run 1&2	**New**
$B^\pm \to DK^{*\pm}$	$D \to h^\pm h'^\mp$	[22]†	Run 1&2	**Updated**
$B^\pm \to DK^{*\pm}$	$D \to h^\pm\pi^\mp\pi^+\pi^-$	[22]†	Run 1&2	**Updated**
$B^\pm \to DK^{*\pm}$	$D \to K^0_S h^+h^-$	[22]†	Run 1&2	**New**
$B^\pm \to Dh^\pm\pi^+\pi^-$	$D \to h^\pm h'^\mp$	[40]	Run 1	*As before*
$B^0 \to DK^{*0}$	$D \to h^\pm h'^\mp$	[23]	Run 1&2	**Updated**
$B^0 \to DK^{*0}$	$D \to h^\pm\pi^\mp\pi^+\pi^-$	[23]	Run 1&2	**Updated**
$B^0 \to DK^{*0}$	$D \to K^0_S h^+h^-$	[24]	Run 1&2	**Updated**
$B^0 \to D^\mp\pi^\pm$	$D^+ \to K^-\pi^+\pi^+$	[41]	Run 1	*As before*
$B^0_s \to D^\mp_s K^\pm$	$D^+_s \to h^+h^-\pi^+$	[25, 42]†	Run 1&2	**Updated**
$B^0_s \to D^\mp_s K^\pm\pi^+\pi^-$	$D^+_s \to h^+h^-\pi^+$	[43]	Run 1&2	*As before*
D decay	Observable(s)	Ref.	Dataset	Status since Ref. [14]
$D^0 \to h^+h^-$	ΔA_{CP}	[44–46]	Run 1&2	*As before*
$D^0 \to K^+K^-$	$A_{CP}(K^+K^-)$	[46–48]	Run 2	*As before*
$D^0 \to h^+h^-$	$y_{CP} - y_{CP}^{K^-\pi^+}$	[49, 50]	Run 1&2	*As before*
$D^0 \to h^+h^-$	ΔY	[51–54]	Run 1&2	*As before*
$D^0 \to K^+\pi^-$ (double tag)	$R^\pm$, $(x'^\pm)^2$, $y'^\pm$	[55]	Run 1	*As before*
$D^0 \to K^+\pi^-$ (single tag)	$R_{K\pi}$, $A_{K\pi}$, $c^{(\prime)}_{K\pi}$, $\Delta c^{(\prime)}_{K\pi}$	[27, 56]	Run 1&2	**Updated**
$D^0 \to K^\pm\pi^\mp\pi^+\pi^-$	$(x^2+y^2)/4$	[57]	Run 1	*As before*
$D^0 \to K^0_S\pi^+\pi^-$	x, y	[58]	Run 1	*As before*
$D^0 \to K^0_S\pi^+\pi^-$	x_{CP}, y_{CP}, Δx, Δy	[59]	Run 1	*As before*
$D^0 \to K^0_S\pi^+\pi^-$	x_{CP}, y_{CP}, Δx, Δy	[60, 61]	Run 2	*As before*
$D^0 \to \pi^+\pi^-\pi^0$	ΔY^{eff}	[26]	Run 2	**New**

† Results presented at ICHEP 2024, but not yet publically available.

Table 2: Auxiliary inputs used in the combination. Those highlighted in bold are new or have changed since the previous combination [14].

Decay	Parameters	Source	Ref.	Status since Ref. [14]
$B^\pm \to DK^{*\pm}$	$\kappa_{B^\pm}^{DK^{*\pm}}$	LHCb	[62]	*As before*
$B^0 \to DK^{*0}$	$\kappa_{B^0}^{DK^{*0}}$	LHCb	[63]	*As before*
$B^0 \to D^\mp\pi^\pm$	β	HFLAV	[13]	**Updated**
$B_s^0 \to D_s^\mp K^\pm(\pi\pi)$	ϕ_s	LHCb	[64]	**Updated**
$D \to K^+\pi^-$	$\cos\delta_D^{K\pi}$, $\sin\delta_D^{K\pi}$, $(r_D^{K\pi})^2$, x^2, y	CLEO-c	[65]	*As before*
$D \to K^+\pi^-$	$A_{K\pi}$, $A_{K\pi}^{\pi\pi^0}$, $r_D^{K\pi}\cos\delta_D^{K\pi}$, $r_D^{K\pi}\sin\delta_D^{K\pi}$	BESIII	[66]	*As before*
$D \to h^+h^-\pi^0$	$F^+_{\pi\pi\pi^0}$, $F^+_{KK\pi^0}$	CLEO-c	[67]	*As before*
$D \to \pi^+\pi^-\pi^+\pi^-$	$F^+_{4\pi}$	CLEO-c+BESIII	[67,68]	*As before*
$D \to K^+K^-\pi^+\pi^-$	$F^+_{KK\pi\pi}$	BESIII	[69]	**New**
$D \to K^+\pi^-\pi^0$	$r_D^{K\pi\pi^0}$, $\delta_D^{K\pi\pi^0}$, $\kappa_D^{K\pi\pi^0}$	CLEO-c+LHCb+BESIII	[70–72]	*As before*
$D \to K^\pm\pi^\mp\pi^+\pi^-$	$r_D^{K3\pi}$, $\delta_D^{K3\pi}$, $\kappa_D^{K3\pi}$	CLEO-c+LHCb+BESIII	[57,70–72]	*As before*
$D \to K_S^0K^\pm\pi^\mp$	$r_D^{K_S^0K\pi}$, $\delta_D^{K_S^0K\pi}$, $\kappa_D^{K_S^0K\pi}$	CLEO-c	[73]	*As before*
$D \to K_S^0K^\pm\pi^\mp$	$r_D^{K_S^0K\pi}$	LHCb	[74]	*As before*

and $D \to K^0_S h^+h^-$ decays [24] as well as results from a time-dependent analysis of $B^0_s \to D^\mp_s K^\pm$ decays [25], which have all been updated to the full LHCb dataset collected during Run 1 and 2.

For the charm inputs, the new result is a measurement of the time-dependent *CP* asymmetry in $D^0 \to \pi^+\pi^-\pi^0$ decays [26], while the updated result is a measurement of mixing and *CP* violation in $D^0 \to K^+\pi^-$ decays [27], which has been updated to the full dataset collected during Run 2. For the latter measurement, the parametrisation in Appendix B of Ref. [27] is employed.

The external constraints include a new measurement of the *CP*-even fraction, F^+, in $D \to K^+K^-\pi^+\pi^-$decays [69], as well as updates to the CKM phases β and ϕ_s from HFLAV [13] and from Ref. [64], respectively.

3 Results

The combination uses a total of 198 input observables to determine 53 free parameters, and the goodness-of-fit is found to be about 20.8%, evaluated using the best-fit χ^2 and cross-checked with simulation. The resulting confidence intervals for each parameter of interest (externally constrained nuisance parameters are not shown) are provided in Table 3. The intervals are computed using a Feldman–Cousins procedure with the *Plugin* treatment of nuisance parameters [75]. Further details of the statistical procedure can be found in Ref. [18]. The correlation matrix is given in Appendix A, while the contribution of each input measurement to the χ^2 is given in Appendix B.

The p-value, or equivalently one minus the confidence level $(1 - \mathrm{CL})$, distribution as a function of γ is shown in Fig. 1 for the total combination and for subcombinations in which the input observables are split by the initial state, final state or analysis method. Confidence intervals for combinations split by initial B state are provided in Table 4. Significant differences between initial state B mesons could be an indication of BSM

Table 3: Confidence intervals and best-fit values for each of the parameters of interest, computed using the Feldman–Cousins *Plugin* method [75]. Entries marked with an asterisk show where the scan has hit a physical boundary.

Quantity	Value	68.3% CL		95.4% CL	
		Uncertainty	Interval	Uncertainty	Interval
$\gamma[^\circ]$	64.6	± 2.8	$[61.8, 67.4]$	$^{+5.5}_{-5.7}$	$[58.9, 70.1]$
$r_{B^\pm}^{DK^\pm}[\%]$	9.73	$^{+0.21}_{-0.20}$	$[9.53, 9.94]$	$^{+0.42}_{-0.40}$	$[9.33, 10.15]$
$\delta_{B^\pm}^{DK^\pm}[^\circ]$	127.4	$^{+2.8}_{-3.0}$	$[124.4, 130.2]$	$^{+5.6}_{-6.2}$	$[121.2, 133.0]$
$r_{B^\pm}^{D\pi^\pm}[\%]$	0.49	$^{+0.06}_{-0.05}$	$[0.44, 0.55]$	$^{+0.12}_{-0.10}$	$[0.39, 0.61]$
$\delta_{B^\pm}^{D\pi^\pm}[^\circ]$	292	$^{+10}_{-11}$	$[281, 301]$	$^{+19}_{-22}$	$[269, 310]$
$r_{B^\pm}^{D^*K^\pm}[\%]$	10.6	± 1.0	$[9.6, 11.6]$	± 2.0	$[8.6, 12.6]$
$\delta_{B^\pm}^{D^*K^\pm}[^\circ]$	312	$^{+6}_{-7}$	$[304, 318]$	$^{+12}_{-16}$	$[296, 324]$
$r_{B^\pm}^{D^*\pi^\pm}[\%]$	0.74	$^{+0.41}_{-0.32}$	$[0.42, 1.15]$	$^{+0.87}_{-0.62}$	$[0.12, 1.61]$
$\delta_{B^\pm}^{D^*\pi^\pm}[^\circ]$	37	$^{+39}_{-20}$	$[17, 76]$	$^{+94}_{-31}$	$[6, 131]$
$r_{B^\pm}^{DK^{*\pm}}[\%]$	10.6	$^{+0.9}_{-1.0}$	$[9.6, 11.5]$	$^{+1.7}_{-2.0}$	$[8.6, 12.3]$
$\delta_{B^\pm}^{DK^{*\pm}}[^\circ]$	49	$^{+14}_{-11}$	$[38, 63]$	$^{+30}_{-23}$	$[26, 79]$
$r_{B^0}^{DK^{*0}}[\%]$	23.4	$^{+1.5}_{-1.6}$	$[21.8, 24.9]$	$^{+2.9}_{-3.3}$	$[20.1, 26.3]$
$\delta_{B^0}^{DK^{*0}}[^\circ]$	192	± 6	$[186, 198]$	$^{+13}_{-12}$	$[180, 205]$
$r_{B_s^0}^{D_s^\mp K^\pm}[\%]$	33.3	$^{+3.7}_{-3.5}$	$[29.8, 37.0]$	$^{+7.5}_{-7.1}$	$[26.2, 40.8]$
$\delta_{B_s^0}^{D_s^\mp K^\pm}[^\circ]$	349	± 6	$[343, 355]$	± 12	$[337, 361]$
$r_{B_s^0}^{D_s^\mp K^\pm\pi^+\pi^-}[\%]$	46	± 8	$[37, 54]$	$^{+16}_{-17}$	$[29, 62]$
$\delta_{B_s^0}^{D_s^\mp K^\pm\pi^+\pi^-}[^\circ]$	345	$^{+13}_{-12}$	$[333, 358]$	$^{+26}_{-25}$	$[320, 371]$
$r_{B^0}^{D^\mp\pi^\pm}[\%]$	3.0	$^{+1.3}_{-1.2}$	$[1.8, 4.3]$	$^{+3.1}_{-2.7}$	$[0.3, 6.1]$
$\delta_{B^0}^{D^\mp\pi^\pm}[^\circ]$	30	$^{+25}_{-36}$	$[-6, 55]$	$^{+45}_{-77}$	$[-47, 75]$
$r_{B^\pm}^{DK^\pm\pi^+\pi^-}[\%]$	8.0	$^{+2.7}_{-3.3}$	$[4.7, 10.7]$	$^{+4.9}_{-8.0}$	$[0.0, 12.9]^*$
$r_{B^\pm}^{D\pi^\pm\pi^+\pi^-}[\%]$	6.2	$^{+2.2}_{-3.0}$	$[3.2, 8.4]$	$^{+3.7}_{-6.2}$	$[0.0, 9.9]^*$
$x[\%]$	0.41	± 0.05	$[0.36, 0.45]$	± 0.09	$[0.31, 0.50]$
$y[\%]$	0.621	$^{+0.022}_{-0.021}$	$[0.600, 0.643]$	$^{+0.044}_{-0.042}$	$[0.579, 0.665]$
$r_D^{K\pi}[\%]$	5.855	$^{+0.010}_{-0.009}$	$[5.846, 5.865]$	$^{+0.020}_{-0.019}$	$[5.836, 5.875]$
$\delta_D^{K\pi}[^\circ]$	191.6	$^{+2.5}_{-2.4}$	$[189.2, 194.1]$	$^{+4.9}_{-5.1}$	$[186.5, 196.5]$
$\lvert q/p\rvert$	0.989	± 0.015	$[0.974, 1.004]$	$^{+0.031}_{-0.030}$	$[0.959, 1.020]$
$\phi[^\circ]$	-2.5	± 1.2	$[-3.7, -1.3]$	± 2.5	$[-5.0, 0.0]$
$a^{\mathrm{d}}_{K^+K^-}[\%]$	0.06	$^{+0.06}_{-0.05}$	$[0.01, 0.12]$	± 0.11	$[-0.05, 0.17]$
$a^{\mathrm{d}}_{\pi^+\pi^-}[\%]$	0.22	± 0.06	$[0.16, 0.28]$	± 0.12	$[0.10, 0.34]$
$a^{\mathrm{d}}_{K^+\pi^-}[\%]$	-0.60	$^{+0.27}_{-0.26}$	$[-0.86, -0.33]$	$^{+0.53}_{-0.54}$	$[-1.14, -0.07]$

Table 4: Confidence intervals and best-fit values for γ when splitting the combination inputs by initial B meson species, computed using the Feldman–Cousins *Plugin* method [75].

Species	Value [°]	68.3% CL		95.4% CL	
		Uncertainty	Interval	Uncertainty	Interval
B^+	63.4	$^{+3.2}_{-3.3}$	$[60.1, 66.6]$	$^{+6.4}_{-6.5}$	$[56.9, 69.8]$
B^0	64.6	$^{+6.5}_{-7.5}$	$[57.1, 71.1]$	$^{+12.0}_{-17.0}$	$[48.0, 77.0]$
B^0_s	75.0	$^{+10.0}_{-11.0}$	$[64.0, 85.0]$	± 20.0	$[55.0, 95.0]$

Table 5: Confidence intervals and best-fit values for γ when splitting the combination inputs by time-dependent and time-integrated methods, computed using the Feldman–Cousins *Plugin* method [75].

Method	Value [°]	68.3% CL		95.4% CL	
		Uncertainty	Interval	Uncertainty	Interval
Time integrated	63.6	± 3.0	$[60.6, 66.6]$	$^{+5.9}_{-6.2}$	$[57.4, 69.5]$
Time dependent	75.0	$^{+10.0}_{-11.0}$	$[64.0, 85.0]$	± 20.0	$[55.0, 95.0]$

effects entering at tree level, as the topologies of the decay amplitudes for charged and neutral initial states are different. Figure 1 shows excellent agreement between all modes. Table 5 presents the confidence intervals for γ determined separately from time-dependent and time-integrated measurements.

Two-dimensional profile-likelihood contours for the charm mixing parameters (x, y), as defined in Ref. [18], and for the $(r_D^{K\pi}, \delta_D^{K\pi})$ parameters are shown in Fig. 2. These demonstrate that the combination of beauty and charm measurements significantly improves the precision on the parameters y and $\delta_D^{K\pi}$. Two-dimensional profile-likelihood contours in the $(a^{\rm d}_{K^+K^-}, a^{\rm d}_{\pi^+\pi^-})$ and $(|q/p|, \phi)$ planes are shown in Fig. 3. The large correlation between $a^{\rm d}_{K^+K^-}$ and $a^{\rm d}_{\pi^+\pi^-}$ follows from the much better precision of the ΔA_{CP} measurement [44] compared to the measurement of the time-integrated CP asymmetry of $D^0 \to K^+K^-$ decays [47].

A breakdown of the sensitivity from different measurements to the parameters of greatest interest is shown in Figs. 4 to 7. These highlight the complementary nature of the input measurements to constrain both γ and the charm mixing parameters. All one-dimensional figures are produced using the *Plugin* treatment [28] of nuisance parameters, while two-dimensional figures are produced using the profile-likelihood method, also known as *Prob* method [28], to limit the usage of computing power.

The determined value of γ from this combination, $(64.6 \pm 2.8)°$, is compatible with the previous LHCb combination, $\gamma = (63.8^{+3.5}_{-3.7})°$ [14], and is in excellent agreement with the global CKM fit predictions. The charm mixing parameters are determined to be $x = (0.41 \pm 0.05)\%$ and $y = (0.621^{+0.022}_{-0.021})\%$. The magnitude and phase of CP violation in charm mixing are determined to be $|q/p| = 0.989 \pm 0.015$ and $\phi = (-2.5 \pm 1.2)°$. Finally, the CP asymmetries in the decay are determined to be $a^{\rm d}_{K^+K^-} = (6^{+6}_{-5}) \times 10^{-4}$ and $a^{\rm d}_{\pi^+\pi^-} = (22 \pm 6) \times 10^{-4}$, with a correlation of $\rho = 0.88$. The change since the last combination [14] is due to the new measurement of $D^0 \to K^+\pi^-$ decays [27], which provides a measurement of the following difference of CP asymmetries, $a^{\rm d}_{K^+\pi^-} - a^{\rm d}_{K^+K^-}$.

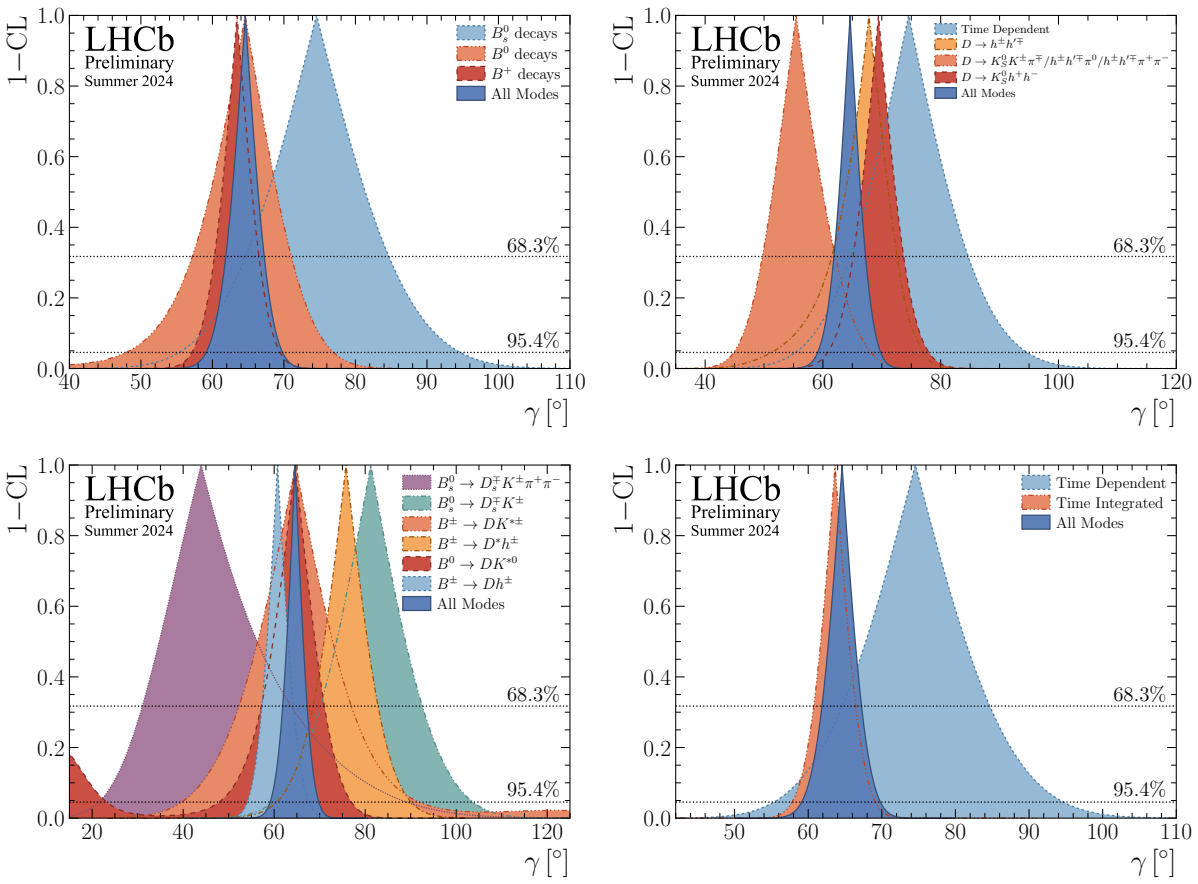

Figure 1: One-dimensional profile-likelihood scans of the $1 - \mathrm{CL}$ distribution for the CKM angle γ. In each plot, the total combination, which includes all beauty and charm modes, is shown in dark blue with a solid line. Top left: inputs split by contributions from B_s^0 (light blue, dotted), B^0 (dark orange, dot-dashed), and B^+ mesons (red, dashed). Top right: inputs split by contributions from time-dependent modes (light blue, dotted), 2-body D decays (light orange, single-dot-dashed), $D \to K_S^0 h^+ h^-$ decays (red, dashed), and other multibody D decays (dark orange, triple-dot-dashed). Bottom left: inputs split by contributions from $B_s^0 \to D_s^\mp K^\pm \pi^+ \pi^-$ (purple, fine-dotted), $B_s^0 \to D_s^\mp K^\pm$ (green, double-dot-dashed), $B^\pm \to DK^{*\pm}$ (dark orange, triple-dot-dashed), $B^\pm \to D^* h^\pm$ (light orange, single-dot-dashed), $B^0 \to DK^{*0}$ (red, dashed), and $B^\pm \to Dh^\pm$ (light blue, dotted) decays. Bottom right: inputs split by contributions from time-dependent (light blue, dotted) and time-integrated (dark orange, dot-dashed) measurements.

The phase $\delta_D^{K\pi}$ is determined to be $(191.6^{+2.5}_{-2.4})^\circ$, increasing the significance of the deviation of its value from the limit of U-spin symmetry ($\delta_D^{K\pi} = 180^\circ$) [76] compared with the previous combination [14]. While the breaking of U-spin symmetry is well established by the measured branching fractions of $D^0 \to K^+\pi^-$ and $D^0 \to K^-\pi^+$ decays [76], more precise determinations of the phase $\delta_D^{K\pi}$ can help clarify the size and nature of the contribution to U-spin breaking from rescattering [77–82] and provide additional information on nonperturbative strong interactions at the charm-mass scale, which limit the precision of the predictions of CP violation in charm decays [83–90].

The relative impact of systematic uncertainties on the input observables is studied, and found to contribute approximately 1.4° to the result for the angle γ, demonstrating that the uncertainties for the combination are still in the regime of statistical dominance.

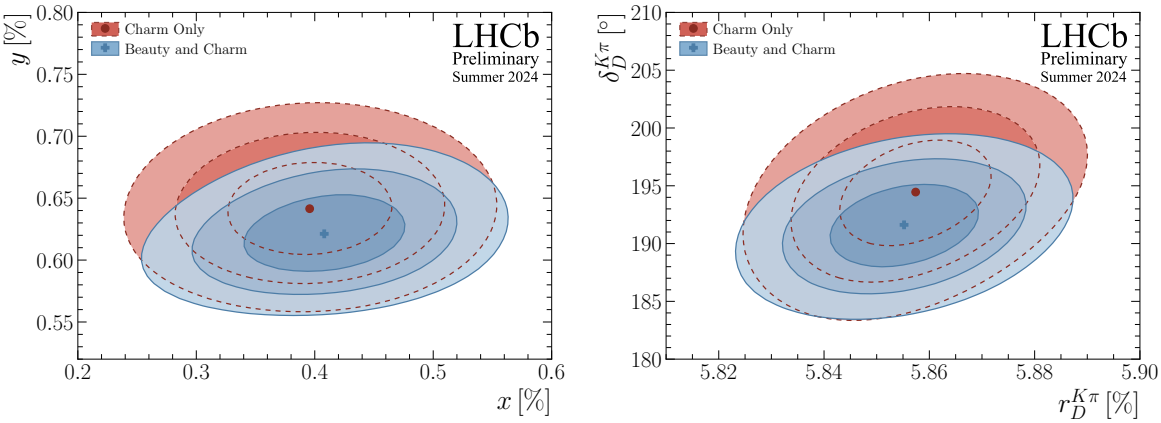

Figure 2: Two-dimensional profile-likelihood contours for (left) the charm mixing parameters x and y, and (right) the $r_D^{K\pi}$ and $\delta_D^{K\pi}$ parameters. The red dashed contours correspond to the combination of only the charm inputs, and the blue solid contours show the result of this combination. Contours are drawn out to 3σ and contain 68.3%, 95.4% and 99.7% of the distribution.

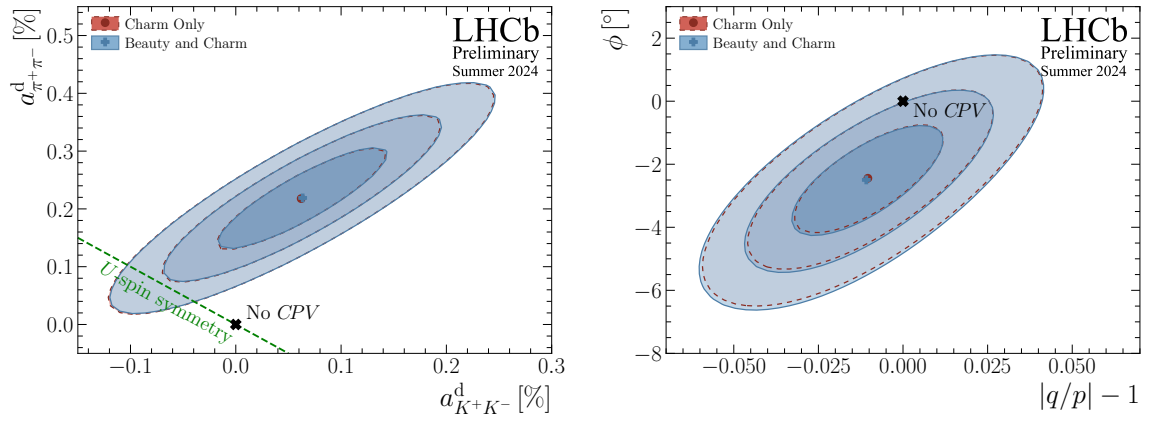

Figure 3: Two-dimensional profile-likelihood contours for (left) the *CP* asymmetries in the decay of the $D^0 \to K^+K^-$ and $D^0 \to \pi^+\pi^-$ channels, and (right) the $|q/p|$ and ϕ parameters. The red dashed contours correspond to the combination of only the charm inputs, which are covered by the blue solid contours showing the result of this combination. Contours are drawn out to 3σ and contain 68.3%, 95.4% and 99.7% of the distribution. The marks labelled with "No *CPV*" identify the scenario without *CP* violation.

The correlated systematic uncertainty due to common inputs used by γ measurements with $D \to K^0_S h^+h^-$ decays are accounted for in the combination, but all other systematic uncertainties from statistically independent measurements are neglected, as this effect is expected to be smaller than 1°. The majority of systematic uncertainties are expected to reduce with additional data.

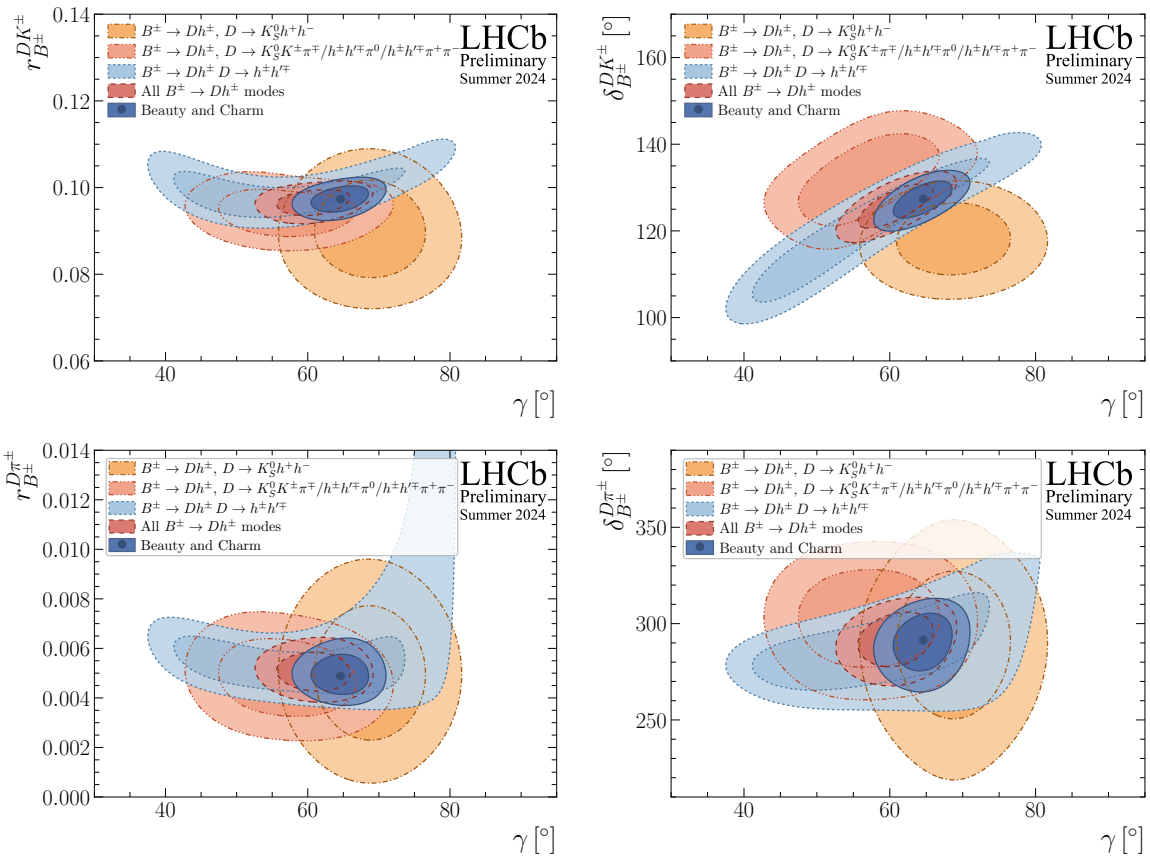

Figure 4: Profile-likelihood contours for the components that contribute towards the γ part of the combination, showing the breakdown of sensitivity amongst different subcombinations of decay modes. The contours shown are the two-dimensional 1σ and 2σ contours, which correspond to the areas containing 68.3% and 95.4% of the distribution.

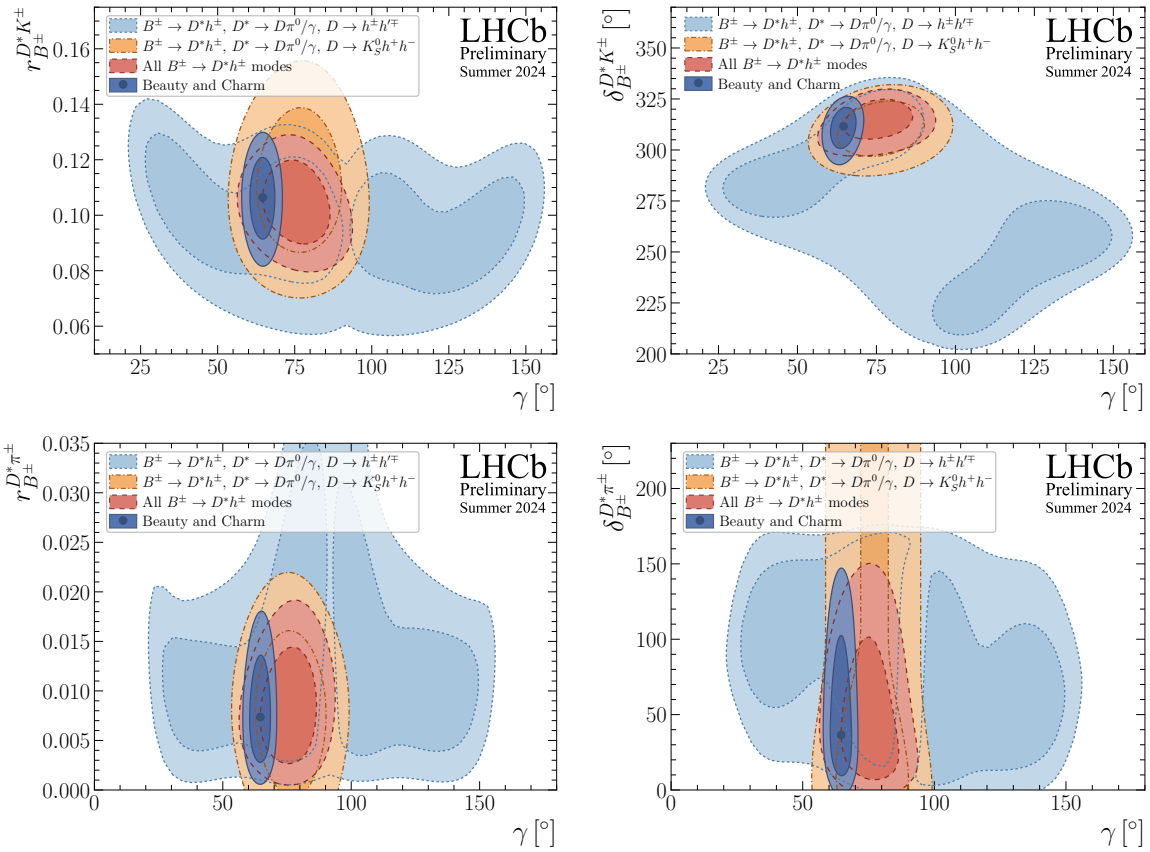

Figure 5: Profile-likelihood contours for the components that contribute towards the γ part of the combination, showing the breakdown of sensitivity amongst different subcombinations of decay modes. The contours shown are the two-dimensional 1σ and 2σ contours, which correspond to the areas containing 68.3% and 95.4% of the distribution.

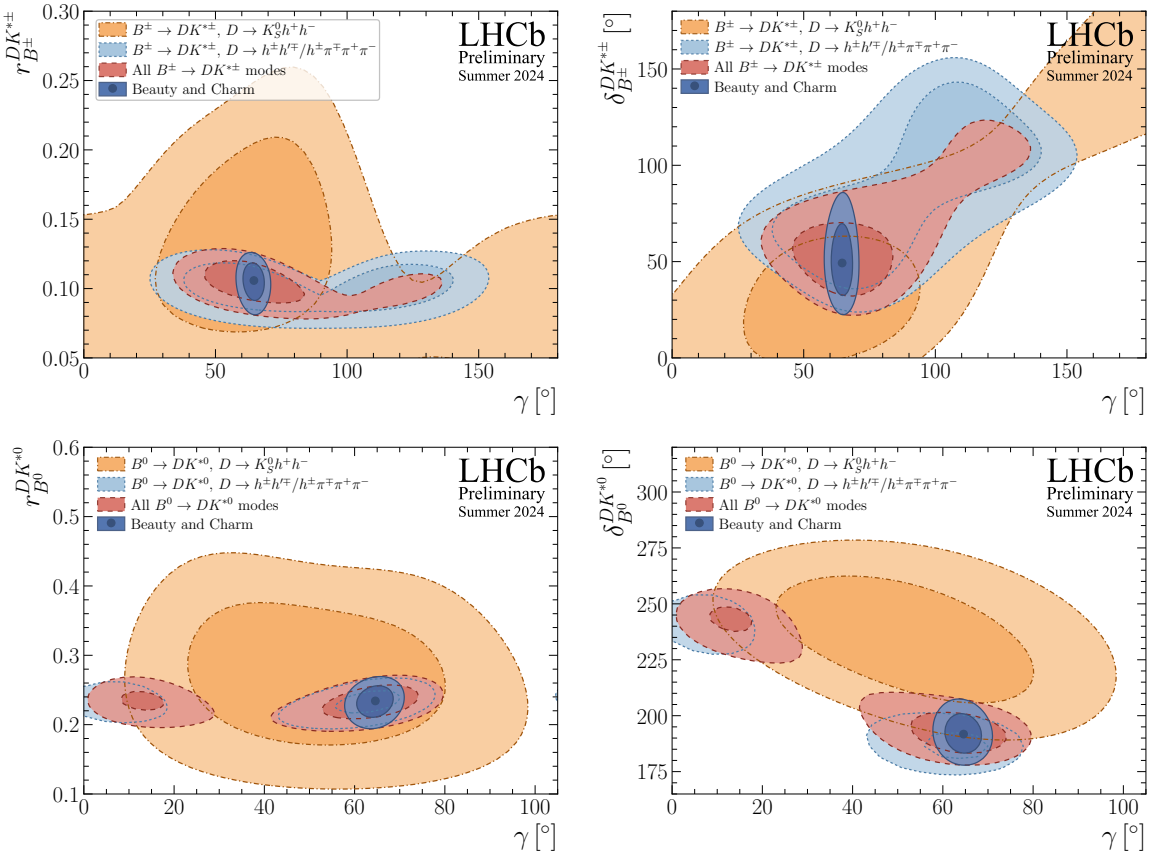

Figure 6: Profile-likelihood contours for the components that contribute towards the γ part of the combination, showing the breakdown of sensitivity amongst different subcombinations of decay modes. The contours shown are the two-dimensional 1σ and 2σ contours, which correspond to the areas containing 68.3% and 95.4% of the distribution.

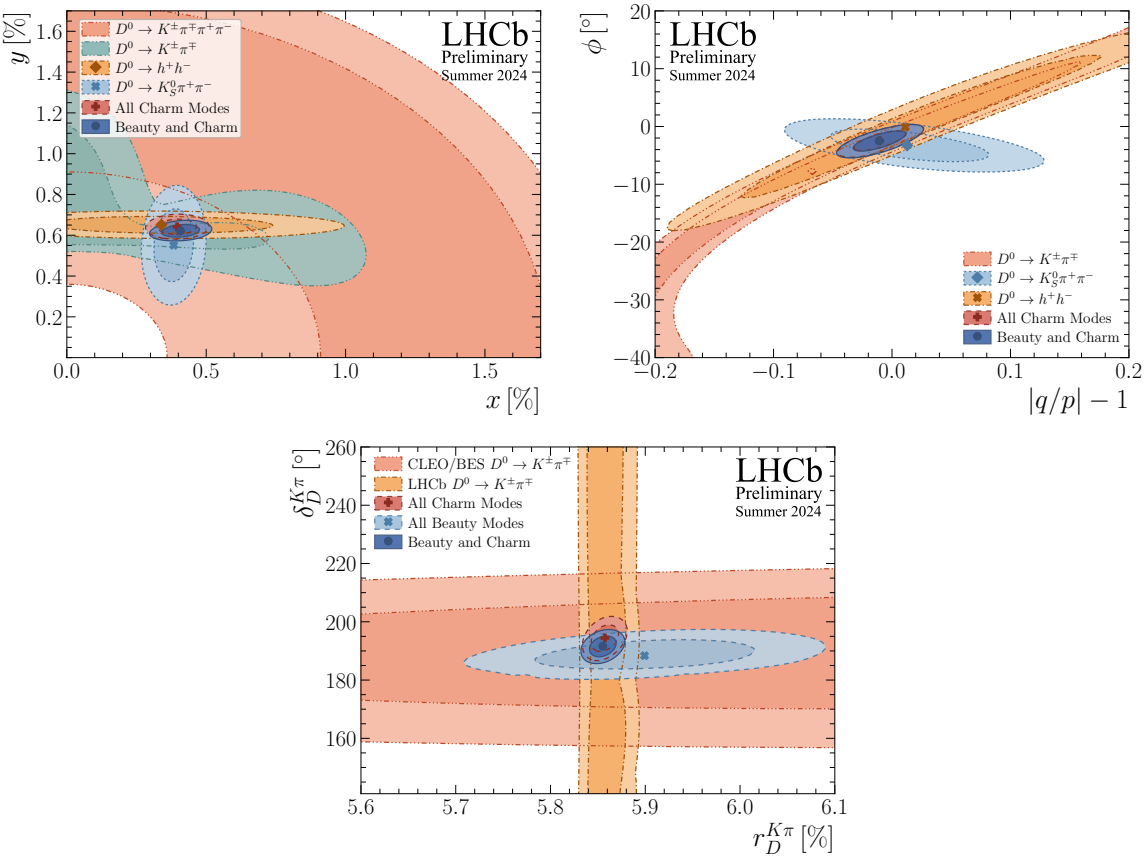

Figure 7: Profile-likelihood contours for the charm decay and mixing parameters, showing the breakdown of sensitivity amongst different decay modes. The contours indicate the 68.3% and 95.4% confidence regions. In the top-right plot, the red contours corresponding to the fit using all charm inputs are hidden below the blue ones that include also beauty inputs, which do not significantly improve the precision. In the top plots, the following parameters are fixed to their best-fit values: $r_D^{K\pi}$, $\delta_D^{K\pi}$, $|q/p|$ and ϕ for the $D^0 \to h^+h^-$ subcombination in the left plot; x and y for all subcombinations, and additionally $r_D^{K\pi}$ and $\delta_D^{K\pi}$ for the $D^0 \to h^+h^-$ subcombination, in the right plot.

4 Results under the assumption of no *CP* violation in doubly Cabibbo-suppressed D^0 decays

For the first time, the fit is repeated also under the assumption of no *CP* violation in doubly Cabibbo-suppressed $D^0 \to K^+\pi^-$ decays, *i.e.* $a^{\rm d}_{K^+\pi^-} = 0$. This condition is expected to hold in the SM within a better precision than that achievable at all current and planned experiments. It allows for better precision to be achieved for the parameters of *CP* violation in D^0 mixing and for the *CP* asymmetries in $D^0 \to h^+h^-$ decays, while having negligible impact on the results for γ and the hadronic parameters of B-meson decays. The corresponding results are shown in Table 6, while a comparison of the results for the charm *CP*-violation parameters with and without this assumption is provided in Fig. 8. The combination uses a total of 197 input observables to determine 52 free parameters, and the goodness-of-fit is found to be about 13.7%, evaluated using the best-fit χ^2.

Table 6: Confidence intervals and best-fit values for each of the parameters of interest, computed using the Feldman–Cousins *Plugin* method [75], for the fit under the assumption of no *CP* violation in doubly Cabibbo-suppressed $D^0 \to K^+\pi^-$ decays ($a^{\rm d}_{K^+\pi^-} = 0$). Only the results for the charm parameters are shown, as the results for the parameters of B decays are indistinguishable from those of Table 3.

Quantity	Value	68.3% CL		95.4% CL	
		Uncertainty	Interval	Uncertainty	Interval
$x[\%]$	0.41	± 0.05	$[0.36, 0.45]$	$^{+0.09}_{-0.10}$	$[0.31, 0.50]$
$y[\%]$	0.619	± 0.021	$[0.598, 0.640]$	$^{+0.044}_{-0.046}$	$[0.573, 0.663]$
$r_D^{K\pi}[\%]$	5.855	$^{+0.009}_{-0.010}$	$[5.845, 5.864]$	$^{+0.019}_{-0.021}$	$[5.834, 5.874]$
$\delta_D^{K\pi}[^\circ]$	191.4	± 2.4	$[189.0, 193.8]$	$^{+4.8}_{-5.0}$	$[186.4, 196.2]$
$\lvert q/p\rvert$	0.984	$^{+0.014}_{-0.015}$	$[0.969, 0.998]$	$^{+0.029}_{-0.030}$	$[0.954, 1.013]$
$\phi[^\circ]$	-1.6	$^{+1.1}_{-1.2}$	$[-2.8, -0.5]$	$^{+2.4}_{-2.8}$	$[-4.4, 0.8]$
$a^{\rm d}_{K^+K^-}[\%]$	0.09	± 0.05	$[0.04, 0.14]$	± 0.11	$[-0.02, 0.20]$
$a^{\rm d}_{\pi^+\pi^-}[\%]$	0.24	± 0.06	$[0.19, 0.30]$	$^{+0.12}_{-0.11}$	$[0.13, 0.36]$

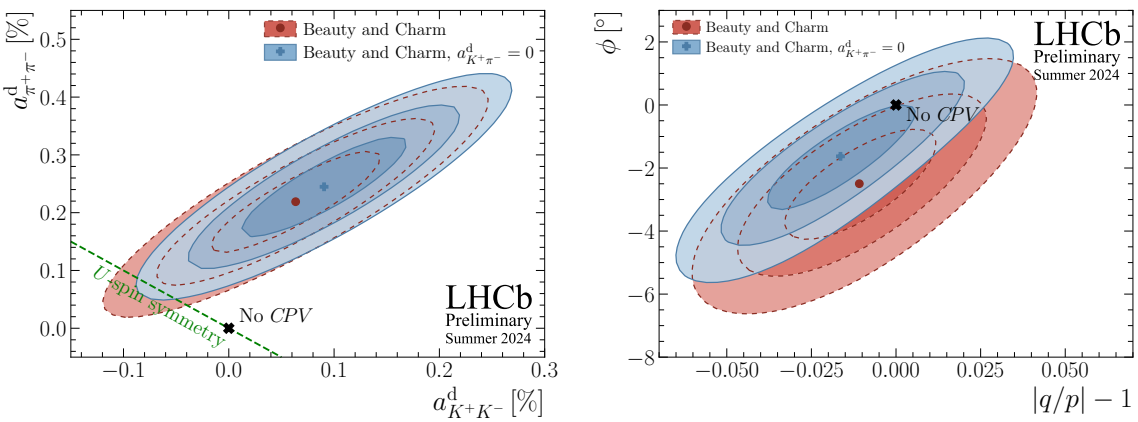

Figure 8: Two-dimensional profile-likelihood contours for (left) the *CP* asymmetries in the decay of the $D^0 \to K^+K^-$ and $D^0 \to \pi^+\pi^-$ channels, and (right) the $|q/p|$ and ϕ parameters. All shown contours employ both the charm and beauty inputs; the red dashed contours correspond to the baseline results, and the blue solid contours show the result of the combination under the assumption of no *CP* violation in doubly Cabibbo-suppressed $D^0 \to K^+\pi^-$ decays. Contours are drawn out to 3σ and contain 68.3%, 95.4% and 99.7% of the distribution. The marks labelled with "No *CPV*" identify the scenario without *CP* violation.

5 Summary

An updated combination of LHCb measurements constraining the CKM angle γ and charm mixing and *CP*-violation parameters has been performed. This combination provides the world's most precise determination of γ from direct measurements to date, finding $\gamma = (64.6 \pm 2.8)^\circ$. Without any assumptions on *CP* violation in the charm system, the charm-mixing and *CP*-violation parameters are determined to be $x = (0.41 \pm 0.05)\%$, $y = (0.621^{+0.022}_{-0.021})\%$, $|q/p| = 0.989 \pm 0.015$, $\phi = (-2.5 \pm 1.2)^\circ$, $a^{d}_{K^+\pi^-} = (-0.60^{+0.27}_{-0.26})\%$, $a^{d}_{K^+K^-} = (6^{+6}_{-5}) \times 10^{-4}$ and $a^{d}_{\pi^+\pi^-} = (22 \pm 6) \times 10^{-4}$. A comparison of the precision of the present combination with previous LHCb determinations of the same parameters is provided in Appendix C. An alternate combination assuming $a^{d}_{K^+\pi^-} = 0$ provides results consistent with the nominal combination, but with improved precision on charm *CP*-violation parameters.

Appendices

A Correlation matrix

A subset of the global fit correlation matrix for the parameters of greatest interest presented in Table 3 is provided in Table 7 and visualised in Fig. 9. The total correlation matrix is given in Table 8 and visualised in Fig. 10.

Table 7: Reduced correlation matrix for the parameters of greater interest. Values smaller than 0.01 are replaced with a "-" symbol.

	γ	$r_{B^\pm}^{DK^\pm}$	$\delta_{B^\pm}^{DK^\pm}$	$r_{B^\pm}^{D\pi^\pm}$	$\delta_{B^\pm}^{D\pi^\pm}$	$r_D^{K\pi}$	$\delta_D^{K\pi}$	x	y	$\lvert q/p\rvert$	ϕ	$a^{\mathrm{d}}_{K^+K^-}$	$a^{\mathrm{d}}_{\pi^+\pi^-}$	$a^{\mathrm{d}}_{K^+\pi^-}$
γ	1.00	0.36	0.62	–0.02	0.19	-	-	-	-	-	-	-	-	-
$r_{B^\pm}^{DK^\pm}$		1.00	0.21	-	0.07	–0.04	–0.10	0.02	–0.08	-	-	-	-	-
$\delta_{B^\pm}^{DK^\pm}$			1.00	–0.04	0.18	–0.11	–0.39	0.06	–0.32	-	–0.01	-	-	0.02
$r_{B^\pm}^{D\pi^\pm}$				1.00	0.57	0.04	0.02	-	0.01	-	-	-	-	-
$\delta_{B^\pm}^{D\pi^\pm}$					1.00	0.01	–0.13	0.02	–0.11	-	-	-	-	-
$r_D^{K\pi}$						1.00	0.29	0.18	–0.07	–0.04	0.01	-	-	–0.02
$\delta_D^{K\pi}$							1.00	–0.05	0.84	-	0.04	–0.02	–0.02	–0.05
x								1.00	0.22	–0.09	0.09	0.01	-	-
y									1.00	–0.04	0.04	–0.01	–0.01	–0.06
$\lvert q/p\rvert$										1.00	0.72	0.11	0.10	–0.16
ϕ											1.00	–0.04	–0.04	0.33
$a^{\mathrm{d}}_{K^+K^-}$												1.00	0.87	0.22
$a^{\mathrm{d}}_{\pi^+\pi^-}$													1.00	0.20
$a^{\mathrm{d}}_{K^+\pi^-}$														1.00

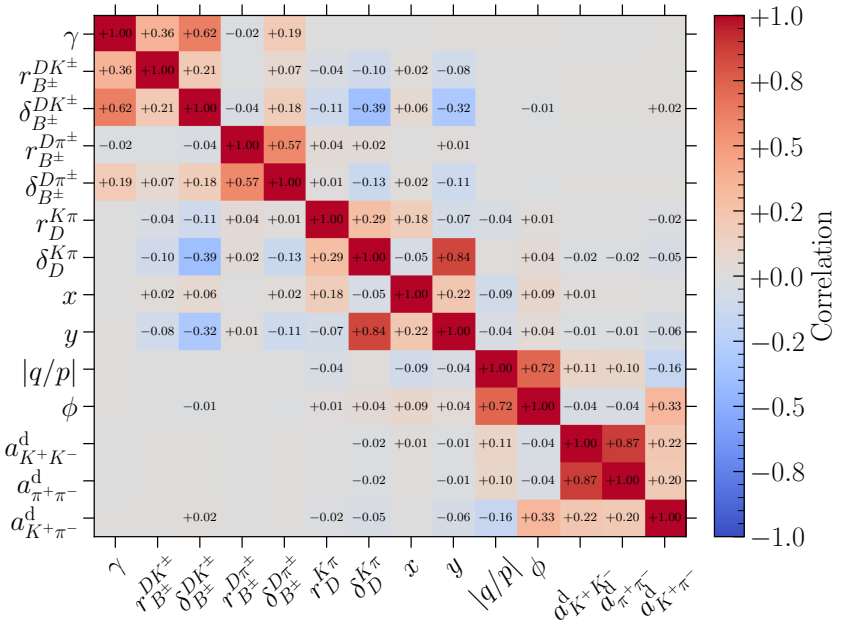

Figure 9: Reduced correlation matrix for the parameters of greatest interest. Values smaller than 0.01 are not written.

Table 8: Correlation matrix of the fit result. Values smaller than 0.01 are replaced with a "-" symbol.

	γ	$r_{B^\pm}^{DK^\pm}$	$\delta_{B^\pm}^{DK^\pm}$	$r_{B^\pm}^{D\pi^\pm}$	$\delta_{B^\pm}^{D\pi^\pm}$	$r_{B^\pm}^{D^*K^\pm}$	$\delta_{B^\pm}^{D^*K^\pm}$	$r_{B^\pm}^{D^*\pi^\pm}$	$\delta_{B^\pm}^{D^*\pi^\pm}$	$r_{B^\pm}^{DK^{*\pm}}$	$\delta_{B^\pm}^{DK^{*\pm}}$	$r_{B^0}^{DK^{*0}}$	$\delta_{B^0}^{DK^{*0}}$	$r_{B_s^0}^{D_s^\mp K^\pm}$	$\delta_{B_s^0}^{D_s^\mp K^\pm}$	$r_{B_s^0}^{D_s^\mp K^\pm\pi^+\pi^-}$	$\delta_{B_s^0}^{D_s^\mp K^\pm\pi^+\pi^-}$	$r_{B^0}^{D^\mp\pi^\pm}$	$\delta_{B^0}^{D^\mp\pi^\pm}$	$r_{B^\pm}^{DK^\pm\pi^+\pi^-}$	$r_{B^\pm}^{D\pi^\pm\pi^+\pi^-}$	$r_D^{K\pi}$	$\delta_D^{K\pi}$	x	y	$\lvert q/p\rvert$	ϕ	$a^{\rm d}_{K^+K^-}$	$a^{\rm d}_{\pi^+\pi^-}$	$a^{\rm d}_{K^+\pi^-}$
γ	1.00	0.36	0.62	−0.02	0.19	-	0.24	0.02	−0.06	−0.12	−0.05	0.16	−0.09	−0.09	−0.06	−0.02	−0.10	−0.05	−0.12	0.02	−0.14	-	-	-	-	-	-	-	-	-
$r_{B^\pm}^{DK^\pm}$		1.00	0.21	-	0.07	-	0.09	0.01	−0.02	−0.03	−0.02	0.06	−0.03	−0.03	−0.02	-	−0.04	−0.02	−0.04	-	−0.02	−0.04	−0.10	0.02	−0.08	-	-	-	-	-
$\delta_{B^\pm}^{DK^\pm}$			1.00	−0.04	0.18	−0.01	0.17	0.02	−0.03	−0.05	−0.03	0.10	−0.05	−0.06	−0.04	−0.01	−0.06	−0.03	−0.08	-	0.03	−0.11	−0.39	0.06	−0.32	-	−0.01	-	-	0.02
$r_{B^\pm}^{D\pi^\pm}$				1.00	0.57	-	-	-	-	-	-	-	-	-	-	-	-	-	-	-	-	0.04	0.02	-	0.01	-	-	-	-	-
$\delta_{B^\pm}^{D\pi^\pm}$					1.00	-	0.05	-	−0.01	−0.01	−0.01	0.03	−0.01	−0.02	−0.01	-	−0.02	-	−0.02	-	0.01	0.01	−0.13	0.02	−0.11	-	-	-	-	-
$r_{B^\pm}^{D^*K^\pm}$						1.00	0.43	0.02	0.09	-	-	-	-	-	-	-	-	-	-	-	-	-	0.03	-	0.03	-	-	-	-	-
$\delta_{B^\pm}^{D^*K^\pm}$							1.00	0.04	0.03	−0.02	−0.01	0.04	−0.02	−0.02	−0.01	-	−0.02	−0.01	−0.03	-	−0.02	−0.01	−0.05	-	−0.04	-	-	-	-	-
$r_{B^\pm}^{D^*\pi^\pm}$								1.00	−0.68	-	-	-	-	-	-	-	-	-	-	-	-	-	−0.02	-	−0.02	-	-	-	-	-
$\delta_{B^\pm}^{D^*\pi^\pm}$									1.00	-	-	−0.01	-	-	-	-	-	-	-	-	0.01	-	−0.02	-	−0.01	-	-	-	-	-
$r_{B^\pm}^{DK^{*\pm}}$										1.00	−0.49	−0.03	0.01	0.01	-	-	0.01	-	0.01	-	0.04	−0.02	−0.06	0.01	−0.05	-	-	-	-	-
$\delta_{B^\pm}^{DK^{*\pm}}$											1.00	-	-	-	-	-	-	-	-	-	-	-	-	-	-	-	-	-	-	-
$r_{B^0}^{DK^{*0}}$												1.00	−0.11	−0.02	−0.01	-	−0.02	-	−0.02	-	−0.03	-	-	-	-	-	-	-	-	-
$\delta_{B^0}^{DK^{*0}}$													1.00	-	-	-	-	-	0.01	-	0.02	-	−0.02	-	−0.02	-	-	-	-	-
$r_{B_s^0}^{D_s^\mp K^\pm}$														1.00	0.01	-	0.01	-	0.01	-	0.01	-	-	-	-	-	-	-	-	-
$\delta_{B_s^0}^{D_s^\mp K^\pm}$															1.00	-	-	-	-	-	-	-	-	-	-	-	-	-	-	-
$r_{B_s^0}^{D_s^\mp K^\pm\pi^+\pi^-}$																1.00	-	-	-	-	-	-	-	-	-	-	-	-	-	-
$\delta_{B_s^0}^{D_s^\mp K^\pm\pi^+\pi^-}$																	1.00	-	0.01	-	0.01	-	-	-	-	-	-	-	-	-
$r_{B^0}^{D^\mp\pi^\pm}$																		1.00	0.48	-	-	-	-	-	-	-	-	-	-	-
$\delta_{B^0}^{D^\mp\pi^\pm}$																			1.00	-	0.02	-	-	-	-	-	-	-	-	-
$r_{B^\pm}^{DK^\pm\pi^+\pi^-}$																				1.00	−0.01	0.01	0.04	-	0.03	-	-	-	-	-
$r_{B^\pm}^{D\pi^\pm\pi^+\pi^-}$																					1.00	−0.08	−0.30	0.05	−0.24	-	-	-	-	0.02
$r_D^{K\pi}$																						1.00	0.29	0.18	−0.07	−0.04	0.01	-	-	−0.02
$\delta_D^{K\pi}$																							1.00	−0.05	0.84	-	0.04	−0.02	−0.02	−0.05
x																								1.00	0.22	−0.09	0.09	0.01	-	-
y																									1.00	−0.04	0.04	−0.01	−0.01	−0.06
$\lvert q/p\rvert$																										1.00	0.72	0.11	0.10	−0.16
ϕ																											1.00	−0.04	−0.04	0.33
$a^{\rm d}_{K^+K^-}$																												1.00	0.87	0.22
$a^{\rm d}_{\pi^+\pi^-}$																													1.00	0.20
$a^{\rm d}_{K^+\pi^-}$																														1.00

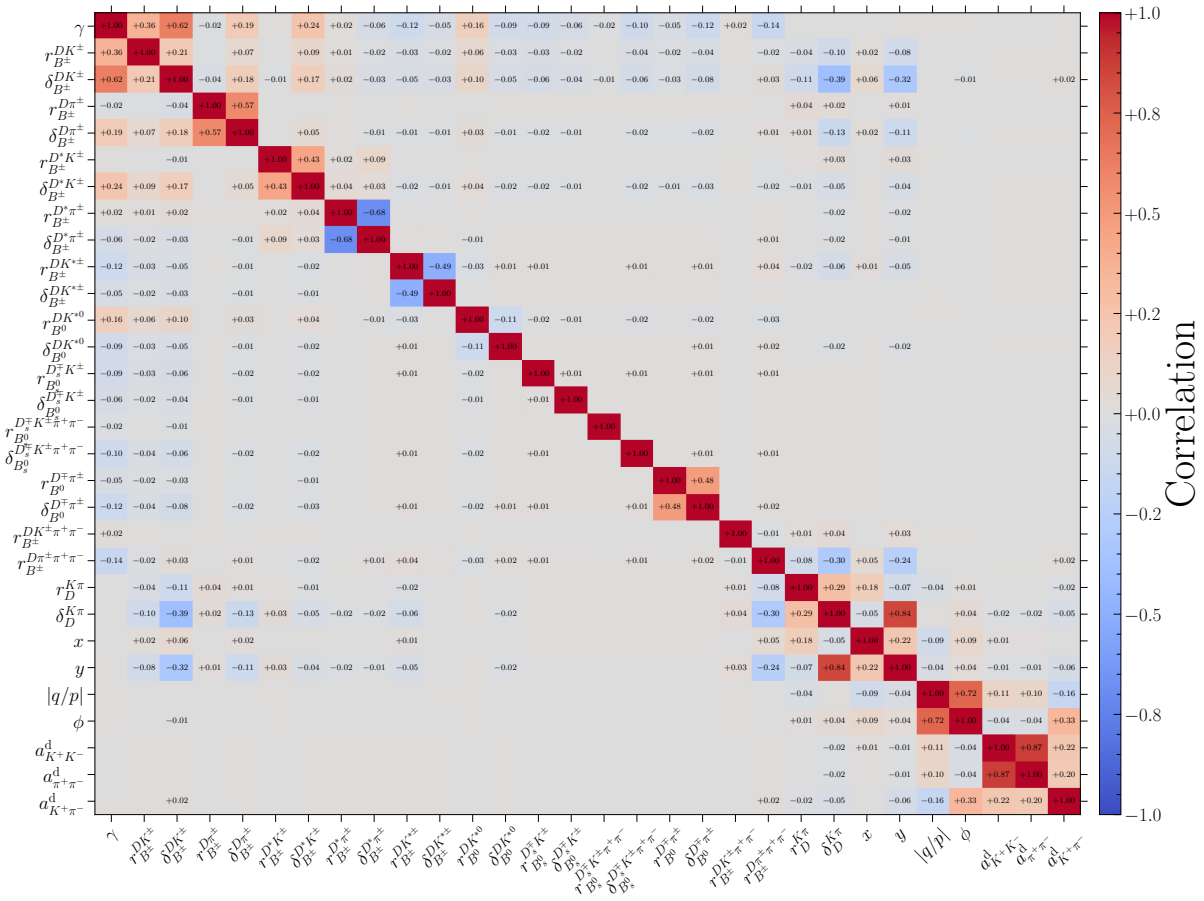

Figure 10: Correlation matrix of the fit result. Values smaller than 0.01 are not written.

B Contribution of each input measurement to the global χ^2

The contribution of each input measurement to the global χ^2 of the baseline fit, where $a^{\rm d}_{K^+\pi^-}$ is free to vary, is shown in Table 9.

Table 9: Contributions to the total χ^2 of the global fit of the baseline fit, where $a^{\rm d}_{K^+\pi^-}$ is free to vary, and number of observables of each input measurement. The global fit contains 53 free parameters.

	Measurement	χ^2	No. of obs.
Beauty sector	$B^\pm \to Dh^\pm, D \to h^\pm h'^\mp$	3.35	8
	GGSZ combined	26.31	26
	$B^\pm \to Dh^\pm, D \to K^0_S K^\pm \pi^\mp$	7.42	7
	$B^\pm \to Dh^\pm, D \to h^\pm h'^\mp \pi^0$	6.06	11
	$B^\pm \to Dh^\pm, D \to K^\pm \pi^\mp \pi^+ \pi^-$	4.75	6
	$B^\pm \to Dh^\pm, D \to h^+ h^- \pi^+ \pi^-$	3.75	6
	$B^\pm \to D^* h^\pm, D \to h^\pm h'^\mp$	9.35	16
	$B^\pm \to DK^{*\pm}, D \to h^\pm h'^\mp (\pi^+\pi^-)$	28.49	12
	$B^0 \to DK^{*0}, D \to h^\pm h'^\mp (\pi^+\pi^-)$	15.08	12
	$B^\pm \to Dh^\pm \pi^+ \pi^-, D \to h^\pm h'^\mp$	1.29	11
	$B^0_s \to D^\mp_s K^\pm$ Run 1	5.39	5
	$B^0_s \to D^\mp_s K^\pm$ Run 2	0.82	5
	$B^0_s \to D^\mp_s K^\pm \pi^+ \pi^-$	2.91	5
	$B^0 \to D^\mp \pi^\pm$	0.00	2
Charm sector	$D \to K^0_S \pi^+ \pi^-$ 2011	5.43	2
	$D \to K^0_S \pi^+ \pi^-$ Run 1	0.87	4
	$D \to K^0_S \pi^+ \pi^-$ Run 2	0.56	4
	$D \to K^\pm \pi^\mp$ (single tag)	2.02	9
	$D \to K^\pm \pi^\mp$ (double tag)	2.63	6
	$\Delta A_{CP},\ A_{CP}(K^+K^-)$	8.52	8
	$D \to K^\pm \pi^\mp \pi^+ \pi^-$	3.61	1
	$D \to h^+ h^-\ y_{CP}$ Run 1	0.33	1
	$D \to h^+ h^-\ y_{CP}$ Run 2	1.46	1
	$D \to h^+ h^-\ \Delta Y$	0.02	1
	$D \to \pi^+ \pi^- \pi^0\ \Delta Y^{\rm eff}$	0.00	1
External constraints	$D \to K^\pm \pi^\mp \pi^0, D \to K^\pm \pi^\mp \pi^+ \pi^-$	0.04	6
	$D \to \pi^+ \pi^- \pi^+ \pi^-$ CLEO-c	1.07	1
	$D \to \pi^+ \pi^- \pi^+ \pi^-$ BESIII	0.40	1
	$D \to K^+ K^- \pi^+ \pi^-$	0.42	1
	$D \to h^+ h^- \pi^0$	0.00	2
	$D \to K^0_S K^\pm \pi^\mp$ Wrong-Sign	0.59	1
	$D \to K^0_S K^\pm \pi^\mp$	3.78	3
	$B^\pm \to DK^{*\pm}$	0.08	1
	$B^0 \to DK^{*0}$	0.00	1
	ϕ_s	0.01	1
	β	0.00	1
	$D \to K^\pm \pi^\mp$ CLEO-c	10.63	5
	$D \to K^\pm \pi^\mp$ BESIII	1.17	4
	Total	158.61	198

C Comparison with the previous combination

A comparison of the sensitivity of this combination with the previous two [14, 18] is provided in Figs. 11 and 12. This combination primarily includes updated γ measurements with Run 1 and 2 data from decay channels other than $B^{\pm} \to Dh^{\pm}$ decays, which allows for significantly improved sensitivity on the hadronic parameters from a number of other decay modes. The updated $B^0 \to DK^{*0}$ measurements from Refs. [23, 24] allow for significant improvement in the determination of γ from B^0 decays, and the updated $B_s^0 \to D_s^{\mp}K^{\pm}$ measurement from Ref. [25] provides significantly improved precision on the determination of γ from B_s^0 decays.

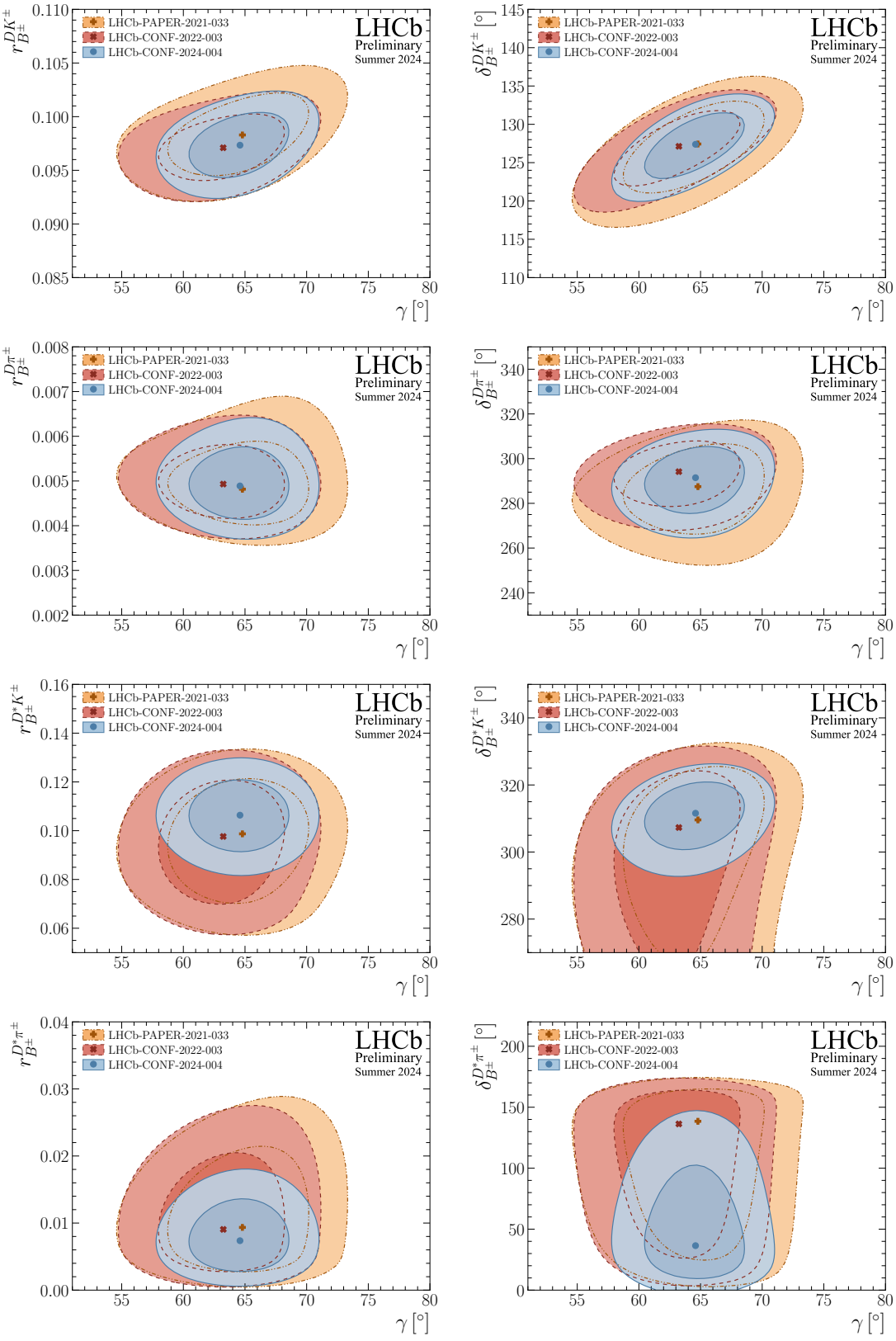

Figure 11: Two-dimensional profile-likelihood contours making a comparison between the previous combinations of Refs. [18] (light orange, dot-dashed) and [14] (red, dashed), and the current one (light blue, solid). The contours shown are the two-dimensional 1σ and 2σ contours which correspond to areas containing 68.3% and 95.4% of the distribution.

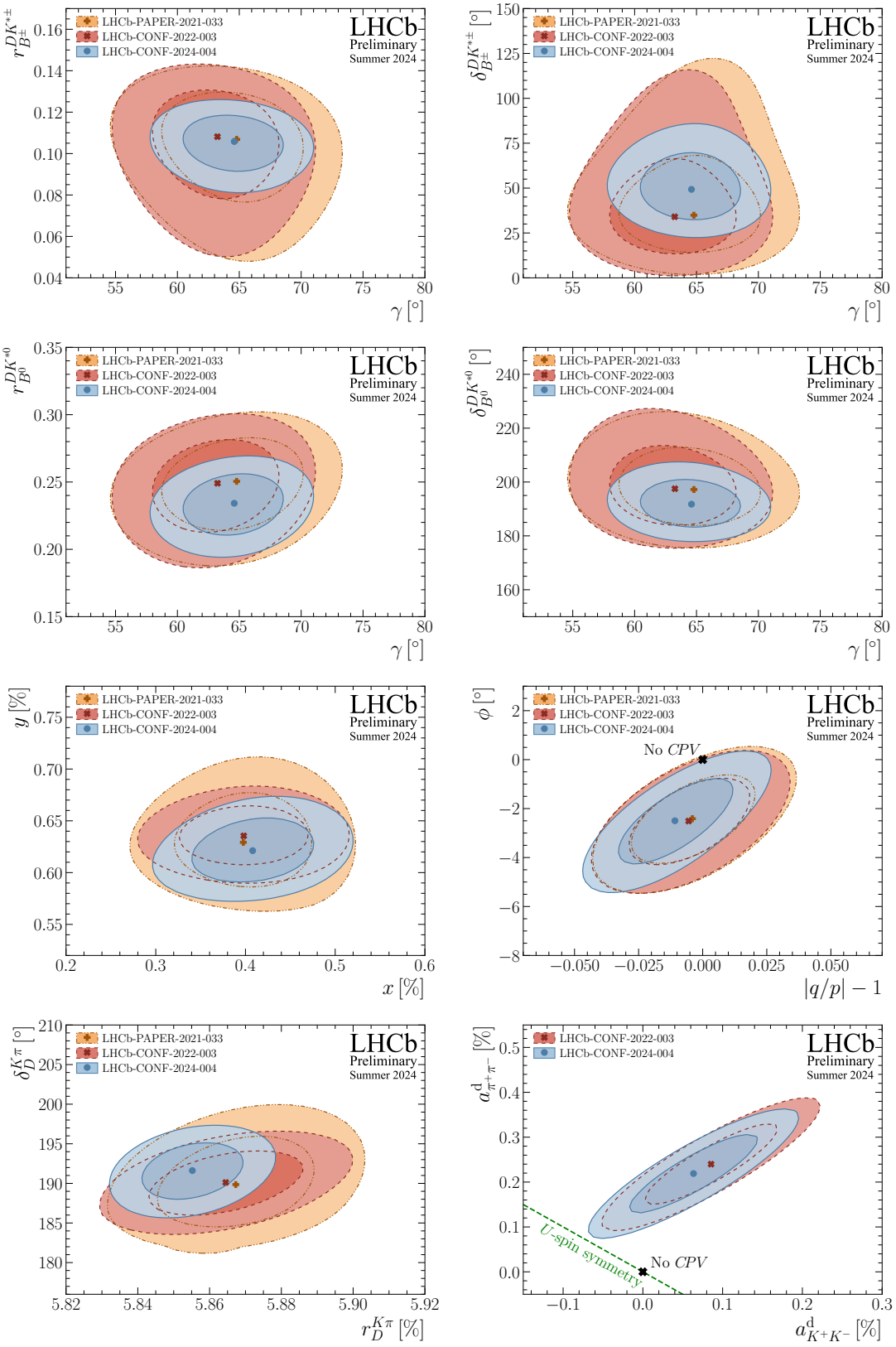

Figure 12: Two-dimensional profile-likelihood contours making a comparison between the previous combinations of Refs. [18] (light orange, dot-dashed) and [14] (red, dashed), and the current one (light blue, solid). The contours shown are the two-dimensional 1σ and 2σ contours which correspond to areas containing 68.3% and 95.4% of the distribution. The marks labelled with "No *CPV*" identify the scenario without *CP* violation.

D Additional plots

A summary of LHCb results for the γ combination as a function of time is given in Fig. 13.

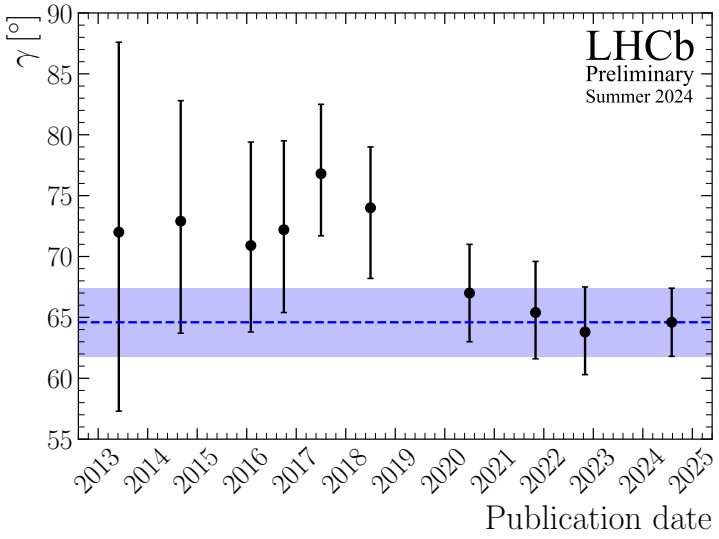

Figure 13: Evolution of published LHCb combination results for γ [14, 18, 28–34], with the best-fit values and uncertainties in black. The result presented in this note is the rightmost data point; its value and uncertainty are highlighted by the dashed blue line and band, respectively.

References

[1] M. Gronau and D. Wyler, *On determining a weak phase from CP asymmetries in charged B decays*, Phys. Lett. **B265** (1991) 172.

[2] M. Gronau and D. London, *How to determine all the angles of the unitarity triangle from $B^0 \to DK^0_S$ and $B^0_s \to D\phi$*, Phys. Lett. **B253** (1991) 483.

[3] D. Atwood, I. Dunietz, and A. Soni, *Enhanced CP violation with $B \to KD^0$ ($\overline{D}^0$) modes and extraction of the Cabibbo–Kobayashi–Maskawa angle γ*, Phys. Rev. Lett. **78** (1997) 3257, arXiv:hep-ph/9612433.

[4] D. Atwood, I. Dunietz, and A. Soni, *Improved methods for observing CP violation in $B^\pm \to KD$ and measuring the CKM phase γ*, Phys. Rev. **D63** (2001) 036005, arXiv:hep-ph/0008090.

[5] A. Bondar, *Proceedings of BINP special analysis meeting on Dalitz analysis*, 24-26 Sep. 2002, unpublished.

[6] A. Giri, Y. Grossman, A. Soffer, and J. Zupan, *Determining γ using $B^\pm \to DK^\pm$ with multibody D decays*, Phys. Rev. **D68** (2003) 054018, arXiv:hep-ph/0303187.

[7] Belle collaboration, A. Poluektov *et al.*, *Measurement of ϕ_3 with Dalitz plot analysis of $B^\pm \to D^{(*)}K^\pm$ decay*, Phys. Rev. **D70** (2004) 072003, arXiv:hep-ex/0406067.

[8] Y. Grossman, Z. Ligeti, and A. Soffer, *Measuring γ in $B^\pm \to K^\pm(KK^*)_D$ decays*, Phys. Rev. **D67** (2003) 071301, arXiv:hep-ph/0210433.

[9] J. Brod, A. Lenz, G. Tetlalmatzi-Xolocotzi, and M. Wiebusch, *New physics effects in tree-level decays and the precision in the determination of the quark mixing angle γ*, Phys. Rev. **D92** (2015) 033002, arXiv:1412.1446.

[10] J. Brod and J. Zupan, *The ultimate theoretical error on γ from $B \to DK$ decays*, JHEP **01** (2014) 051, arXiv:1308.5663.

[11] CKMfitter group, J. Charles *et al.*, *Current status of the standard model CKM fit and constraints on $\Delta F = 2$ new physics*, Phys. Rev. **D91** (2015) 073007, arXiv:1501.05013, updated results and plots available at http://ckmfitter.in2p3.fr/.

[12] UTfit collaboration, M. Bona *et al.*, *The unitarity triangle fit in the standard model and hadronic parameters from lattice QCD: A reappraisal after the measurements of Δm_s and $BR(B \to \tau\nu_\tau)$*, JHEP **10** (2006) 081, arXiv:hep-ph/0606167, updated results and plots available at http://www.utfit.org/.

[13] Y. Amhis *et al.*, *Averages of b-hadron, c-hadron, and τ-lepton properties as of 2021*, Phys. Rev. **D107** (2023) 052008, arXiv:2206.07501, updated results and plots available at https://hflav.web.cern.ch.

[14] LHCb collaboration, *Simultaneous determination of the CKM angle γ and parameters related to mixing and CP violation in the charm sector*, LHCb-CONF-2022-003, 2022.

[15] UTfit collaboration, M. Bona *et al.*, *New UTfit analysis of the unitarity triangle in the Cabibbo–Kobayashi–Maskawa scheme*, Rend. Lincei Sci. Fis. Nat. **34** (2023) 37, arXiv:2212.03894.

[16] LHCb collaboration, *Letter of Intent for the LHCb Upgrade*, CERN-LHCC-2011-001, 2011.

[17] LHCb collaboration, *Physics case for an LHCb Upgrade II — Opportunities in flavour physics, and beyond, in the HL-LHC era*, arXiv:1808.08865.

[18] LHCb collaboration, R. Aaij *et al.*, *Simultaneous determination of CKM angle γ and charm mixing parameters*, JHEP **12** (2021) 141, arXiv:2110.02350.

[19] LHCb collaboration, R. Aaij *et al.*, *A study of CP violation in the decays $B^\pm \to [K^+K^-\pi^+\pi^-]_D h^\pm$ ($h = K, \pi$) and $B^\pm \to [\pi^+\pi^-\pi^+\pi^-]_D h^\pm$*, Eur. Phys. J. **C84** (2023) 547, arXiv:2301.10328.

[20] LHCb collaboration, R. Aaij *et al.*, *A model-independent measurement of the CKM angle γ in partially reconstructed $B^\pm \to D^* h^\pm$ decays with $D \to K^0_S h^+ h^-$ ($h = \pi, K$)*, JHEP **02** (2024) 118, arXiv:2311.10434.

[21] LHCb collaboration, R. Aaij *et al.*, *Measurement of the CKM angle γ using the $B^\pm \to D^* h^\pm$ channels*, JHEP **12** (2023) 013, arXiv:2310.04277.

[22] LHCb collaboration, R. Aaij *et al.*, *Measurement of the CKM angle γ in $B^\pm \to DK^{*\pm}$*, LHCb-PAPER-2024-023, in preparation, to be submitted to JHEP.

[23] LHCb collaboration, R. Aaij *et al.*, *Study of CP violation in $B^0_{(s)} \to DK^*(892)^0$ decays with $D \to K\pi(\pi\pi)$, $\pi\pi(\pi\pi)$, and KK final states*, JHEP **05** (2024) 025, arXiv:2401.17934.

[24] LHCb collaboration, R. Aaij *et al.*, *Measurement of the CKM angle γ in the $B^0 \to D^0K^{*0}$ channel using self-conjugate $D^0 \to K^0_S h^+h^-$ decays*, Eur. Phys. J. **C84** (2024) 206, arXiv:2309.05514.

[25] LHCb collaboration, R. Aaij *et al.*, *Measurement of CP asymmetry in $B^0_s \to D^\mp_s K^\pm$ decays*, LHCb-PAPER-2024-020, in preparation, to be submitted to JHEP.

[26] LHCb collaboration, R. Aaij *et al.*, *Search for time-dependent CP violation in $D^0 \to \pi^+\pi^-\pi^0$ decays*, arXiv:2405.06556, submitted to Phys. Rev. Lett.

[27] LHCb collaboration, R. Aaij *et al.*, *Measurement of D^0–$\overline{D}^0$ mixing and search for CP violation with $D^0 \to K^+\pi^-$ decays*, arXiv:2407.18001, submitted to Phys. Rev. D.

[28] LHCb collaboration, R. Aaij *et al.*, *Measurement of the CKM angle γ from a combination of $B^\pm \to Dh^\pm$ analyses*, Phys. Lett. **B726** (2013) 151, arXiv:1305.2050.

[29] LHCb collaboration, *Improved constraints on γ: CKM2014 update*, LHCb-CONF-2014-004, 2014.

[30] LHCb collaboration, *LHCb γ combination update from $B \to DKX$ decays*, LHCb-CONF-2016-001, 2016.

[31] LHCb collaboration, R. Aaij *et al.*, *Measurement of the CKM angle γ from a combination of LHCb results*, JHEP **12** (2016) 087, arXiv:1611.03076.

[32] LHCb collaboration, *Measurement of the CKM angle γ from a combination of $B \to DK$ analyses*, LHCb-CONF-2017-004, 2017.

[33] LHCb collaboration, *Update of the LHCb combination of the CKM angle γ using $B \to DK$ decays*, LHCb-CONF-2018-002, 2018.

[34] LHCb collaboration, *Updated LHCb combination of the CKM angle γ*, LHCb-CONF-2020-003, 2020.

[35] LHCb collaboration, R. Aaij *et al.*, *Measurement of CP observables in $B^\pm \to D^{(*)}K^\pm$ and $B^\pm \to D^{(*)}\pi^\pm$ decays using two-body D final states*, JHEP **04** (2021) 081, arXiv:2012.09903.

[36] LHCb collaboration, R. Aaij *et al.*, *Measurement of the CKM angle γ with $B^\mp \to D[K^\pm\pi^\mp\pi^\mp\pi^\pm]h^\mp$ decays using a binned phase-space approach*, JHEP **07** (2023) 138, arXiv:2209.03692.

[37] LHCb collaboration, R. Aaij *et al.*, *Constraints on the CKM angle γ from $B^\pm \to Dh^\pm$ decays using $D \to h^\pm h'^\mp\pi^0$ final states*, JHEP **07** (2022) 099, arXiv:2112.10617.

[38] LHCb collaboration, R. Aaij *et al.*, *Measurement of the CKM angle γ in $B^\pm \to DK^\pm$ and $B^\pm \to D\pi^\pm$ decays with $D \to K^0_S h^+ h^-$*, JHEP **02** (2021) 0169, arXiv:2010.08483.

[39] LHCb collaboration, R. Aaij *et al.*, *Measurement of CP observables in $B^\pm \to DK^\pm$ and $B^\pm \to D\pi^\pm$ with $D \to K^0_S K^\pm \pi^\mp$ decays*, JHEP **06** (2020) 58, arXiv:2002.08858.

[40] LHCb collaboration, R. Aaij *et al.*, *Study of $B^- \to DK^-\pi^+\pi^-$ and $B^- \to D\pi^-\pi^+\pi^-$ decays and determination of the CKM angle γ*, Phys. Rev. **D92** (2015) 112005, arXiv:1505.07044.

[41] LHCb collaboration, R. Aaij *et al.*, *Measurement of CP violation in $B^0 \to D^\pm \pi^\mp$ decays*, JHEP **06** (2018) 084, arXiv:1805.03448.

[42] LHCb collaboration, R. Aaij *et al.*, *Measurement of CP asymmetry in $B^0_s \to D^\mp_s K^\pm$ decays*, JHEP **03** (2018) 059, arXiv:1712.07428.

[43] LHCb collaboration, R. Aaij *et al.*, *Measurement of the CKM angle γ and B^0_s-$\overline{B}^0_s$ mixing frequency with $B^0_s \to D^\mp_s h^\pm \pi^\pm \pi^\mp$ decays*, JHEP **03** (2021) 137, arXiv:2011.12041.

[44] LHCb collaboration, R. Aaij *et al.*, *Observation of CP violation in charm decays*, Phys. Rev. Lett. **122** (2019) 211803, arXiv:1903.08726.

[45] LHCb collaboration, R. Aaij *et al.*, *Measurement of the difference of time-integrated CP asymmetries in $D^0 \to K^-K^+$ and $D^0 \to \pi^-\pi^+$ decays*, Phys. Rev. Lett. **116** (2016) 191601, arXiv:1602.03160.

[46] LHCb collaboration, R. Aaij *et al.*, *Measurement of CP asymmetry in $D^0 \to K^-K^+$ and $D^0 \to \pi^-\pi^+$ decays*, JHEP **07** (2014) 041, arXiv:1405.2797.

[47] LHCb collaboration, R. Aaij *et al.*, *Measurement of the time-integrated CP asymmetry in $D^0 \to K^-K^+$ decays*, Phys. Rev. Lett. **131** (2023) 091802, arXiv:2209.03179.

[48] LHCb collaboration, R. Aaij *et al.*, *Measurement of CP asymmetry in $D^0 \to K^-K^+$ decays*, Phys. Lett. **B767** (2017) 177, arXiv:1610.09476.

[49] LHCb collaboration, R. Aaij *et al.*, *Measurement of the charm-mixing parameter y_{CP}*, Phys. Rev. Lett. **122** (2019) 011802, arXiv:1810.06874.

[50] LHCb collaboration, R. Aaij *et al.*, *Measurement of the charm mixing parameter $y_{CP} - y^{K\pi}_{CP}$ using two-body D^0 meson decays*, Phys. Rev. **D105** (2022) 092013, arXiv:2202.09106.

[51] LHCb collaboration, R. Aaij *et al.*, *Measurement of indirect CP asymmetries in $D^0 \to K^-K^+$ and $D^0 \to \pi^-\pi^+$ decays using semileptonic B decays*, JHEP **04** (2015) 043, arXiv:1501.06777.

[52] LHCb collaboration, R. Aaij *et al.*, *Measurement of the CP violation parameter A_Γ in $D^0 \to K^+K^-$ and $D^0 \to \pi^+\pi^-$ decays*, Phys. Rev. Lett. **118** (2017) 261803, arXiv:1702.06490.

[53] LHCb collaboration, R. Aaij *et al.*, *Updated measurement of decay-time-dependent CP asymmetries in $D^0 \to K^+K^-$ and $D^0 \to \pi^+\pi^-$ decays*, Phys. Rev. **D101** (2020) 012005, arXiv:1911.01114.

[54] LHCb collaboration, R. Aaij *et al.*, *Search for time-dependent CP violation in $D^0 \to K^+K^-$ and $D^0 \to \pi^+\pi^-$ decays*, Phys. Rev. **D104** (2021) 072010, arXiv:2105.09889.

[55] LHCb collaboration, R. Aaij *et al.*, *Measurements of charm mixing and CP violation using $D^0 \to K^\pm\pi^\mp$ decays*, Phys. Rev. **D95** (2017) 052004, Erratum ibid. **D96** (2017) 099907, arXiv:1611.06143.

[56] LHCb collaboration, R. Aaij *et al.*, *Updated determination of D^0–$\overline{D}^0$ mixing and CP violation parameters with $D^0 \to K^+\pi^-$ decays*, Phys. Rev. **D97** (2018) 031101, arXiv:1712.03220.

[57] LHCb collaboration, R. Aaij *et al.*, *First observation of $D^0 - \overline{D}^0$ oscillations in $D^0 \to K^+\pi^+\pi^-\pi^-$ decays and a measurement of the associated coherence parameters*, Phys. Rev. Lett. **116** (2016) 241801, arXiv:1602.07224.

[58] LHCb collaboration, R. Aaij *et al.*, *Model-independent measurement of mixing parameters in $D^0 \to K^0_S\pi^+\pi^-$ decays*, JHEP **04** (2016) 033, arXiv:1510.01664.

[59] LHCb collaboration, R. Aaij *et al.*, *Measurement of the mass difference between neutral charm-meson eigenstates*, Phys. Rev. Lett. **122** (2019) 231802, arXiv:1903.03074.

[60] LHCb collaboration, R. Aaij *et al.*, *Observation of the mass difference between neutral charm-meson eigenstates*, Phys. Rev. Lett. **127** (2021) 111801, Erratum ibid. **131** (2023) 079901, arXiv:2106.03744.

[61] LHCb collaboration, R. Aaij *et al.*, *Model-independent measurement of charm mixing parameters in $\overline{B} \to D^0(\to K^{*0}\pi^+\pi^-)\mu^-\overline{\nu}_\mu X$ decays*, Phys. Rev. **D108** (2023) 052005, arXiv:2208.06512.

[62] LHCb collaboration, R. Aaij *et al.*, *Measurement of CP observables in $B^\pm \to DK^{*\pm}$ decays using two- and four-body D-meson final states*, JHEP **11** (2017) 156, Erratum ibid. **05** (2018) 067, arXiv:1709.05855.

[63] LHCb collaboration, R. Aaij *et al.*, *Constraints on the unitarity triangle angle γ from Dalitz plot analysis of $B^0 \to DK^+\pi^-$ decays*, Phys. Rev. **D93** (2016) 112018, Erratum ibid. **D94** (2016) 079902, arXiv:1602.03455.

[64] LHCb collaboration, R. Aaij *et al.*, *Improved measurement of CP violation parameters in $B^0_s \to J/\psi K^+K^-$ decays in the vicinity of the $\phi(1020)$ resonance*, Phys. Rev. Lett. **132** (2024) 051802, arXiv:2308.01468.

[65] CLEO collaboration, D. M. Asner *et al.*, *Updated measurement of the strong phase in $D^0 \to K^+\pi^-$ decay using quantum correlations in $e^+e^- \to D^0\overline{D}^0$ at CLEO*, Phys. Rev. **D86** (2012) 112001, arXiv:1210.0939.

[66] BESIII collaboration, M. Ablikim *et al.*, *Improved measurement of the strong-phase difference $\delta_D^{K\pi}$ in quantum-correlated $D\bar{D}$ decays*, Eur. Phys. J. **C82** (2022) 1009, arXiv:2208.09402.

[67] S. Malde *et al.*, *First determination of the CP content of $D \to \pi^+\pi^-\pi^+\pi^-$ and updated determination of the CP contents of $D \to \pi^+\pi^-\pi^0$ and $D \to K^+K^-\pi^0$*, Phys. Lett. **B747** (2015) 9, arXiv:1504.05878.

[68] BESIII collaboration, M. Ablikim *et al.*, *Measurement of the CP-even fraction of $D^0 \to \pi^+\pi^-\pi^+\pi^-$*, Phys. Rev. **D106** (2022) 092004, arXiv:2208.10098.

[69] BESIII collaboration, M. Ablikim *et al.*, *Measurement of the CP-even fraction of $D^0 \to K^+K^-\pi^+\pi^-$*, Phys. Rev. **D107** (2023) 032009, arXiv:2212.06489.

[70] J. Libby *et al.*, *New determination of the $D^0 \to K^-\pi^+\pi^0$ and $D^0 \to K^-\pi^+\pi^+\pi^-$ coherence factors and average strong-phase differences*, Phys. Lett. **B731** (2014) 197, arXiv:1401.1904.

[71] T. Evans *et al.*, *Improved determination of the $D \to K^-\pi^+\pi^+\pi^-$ coherence factor and associated hadronic parameters from a combination of $e^+e^- \to \psi(3770) \to c\bar{c}$ and $pp \to c\bar{c}X$ data*, Phys. Lett. **B757** (2016) 520, Erratum ibid. **B765** (2017) 402, arXiv:1602.07430.

[72] BESIII collaboration, M. Ablikim *et al.*, *Measurement of the $D \to K^-\pi^+\pi^+\pi^-$ and $D \to K^-\pi^+\pi^0$ coherence factors and average strong-phase differences in quantum-correlated $D\bar{D}$ decays*, JHEP **05** (2021) 164, arXiv:2103.05988.

[73] CLEO collaboration, J. Insler *et al.*, *Studies of the decays $D^0 \to K^0_S K^-\pi^+$ and $D^0 \to K^0_S K^+\pi^-$*, Phys. Rev. **D85** (2012) 092016, Erratum ibid. **D94** (2016) 099905, arXiv:1203.3804.

[74] LHCb collaboration, R. Aaij *et al.*, *Studies of the resonance structure in $D^0 \to K^0_S K^\pm\pi^\mp$ decays*, Phys. Rev. **D93** (2016) 052018, arXiv:1509.06628.

[75] S. Bodhisattva, M. Walker, and M. Woodroofe, *On the unified method with nuisance parameters*, Statist. Sinica **19** (2009) 301.

[76] J. Brod, Y. Grossman, A. L. Kagan, and J. Zupan, *A consistent picture for large penguins in $D \to \pi^+\pi^-$, K^+K^-*, JHEP **10** (2012) 161, arXiv:1203.6659.

[77] L.-L. Chau and H.-Y. Cheng, *SU(3) breaking effects in charmed meson decays*, Phys. Lett. **B333** (1994) 514, arXiv:hep-ph/9404207.

[78] F. Buccella *et al.*, *Nonleptonic weak decays of charmed mesons*, Phys. Rev. **D51** (1995) 3478, arXiv:hep-ph/9411286.

[79] T. E. Browder and S. Pakvasa, *Experimental implications of large CP violation and final state interactions in the search for D^0–$\overline{D}^0$ mixing*, Phys. Lett. **B383** (1996) 475, arXiv:hep-ph/9508362.

[80] A. F. Falk, Y. Nir, and A. A. Petrov, *Strong phases and D^0–$\overline{D}^0$ mixing parameters*, JHEP **12** (1999) 019, arXiv:hep-ph/9911369.

[81] D.-N. Gao, *Strong phases, asymmetries, and SU(3) symmetry breaking in $D \to K\pi$ decays*, Phys. Lett. **B645** (2007) 59, arXiv:hep-ph/0610389.

[82] F. Buccella, A. Paul, and P. Santorelli, *$SU(3)_F$ breaking through final state interactions and CP asymmetries in $D \to PP$ decays*, Phys. Rev. **D99** (2019) 113001, arXiv:1902.05564.

[83] E. Franco, S. Mishima, and L. Silvestrini, *The Standard Model confronts CP violation in $D^0 \to \pi^+\pi^-$ and $D^0 \to K^+K^-$*, JHEP **05** (2012) 140, arXiv:1203.3131.

[84] A. Khodjamirian and A. A. Petrov, *Direct CP asymmetry in $D \to \pi^-\pi^+$ and $D \to K^-K^+$ in QCD-based approach*, Phys. Lett. **B774** (2017) 235, arXiv:1706.07780.

[85] M. Chala, A. Lenz, A. V. Rusov, and J. Scholtz, *ΔA_{CP} within the Standard Model and beyond*, JHEP **07** (2019) 161, arXiv:1903.10490.

[86] Y. Grossman and S. Schacht, *The emergence of the $\Delta U = 0$ rule in charm physics*, JHEP **07** (2019) 020, arXiv:1903.10952.

[87] S. Schacht and A. Soni, *Enhancement of charm CP violation due to nearby resonances*, Phys. Lett. **B825** (2022) 136855, arXiv:2110.07619.

[88] A. Pich, E. Solomonidi, and L. Vale Silva, *Final-state interactions in the CP asymmetries of charm-meson two-body decays*, Phys. Rev. **D108** (2023) 036026, arXiv:2305.11951.

[89] M. Gavrilova, Y. Grossman, and S. Schacht, *Determination of the $D \to \pi\pi$ ratio of penguin over tree diagrams*, Phys. Rev. **D109** (2024) 033011, arXiv:2312.10140.

[90] A. Lenz, M. L. Piscopo, and A. V. Rusov, *Two body non-leptonic D^0 decays from LCSR and implications for $\Delta a_{CP}^{\rm dir}$*, JHEP **03** (2024) 151, arXiv:2312.13245.